

# Synthesis and Evaluation of $^{68}\text{Ga}$ - and $^{177}\text{Lu}$ -Labeled (*R*)- vs (*S*)-DOTAGA Prostate-Specific Membrane Antigen-Targeting Derivatives

Ruiyue Zhao, Karl Ploessl, Zhihao Zha, Seokrye Choi, David Alexoff, Lin Zhu, and Hank F. Kung\*

Cite This: <https://dx.doi.org/10.1021/acs.molpharmaceut.0c00777>

Read Online

ACCESS |

Metrics & More

Article Recommendations

Supporting Information

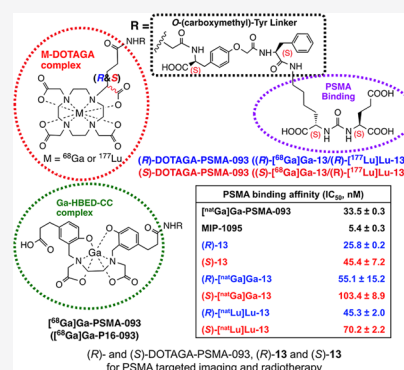
**ABSTRACT:** Prostate-specific membrane antigen (PSMA) is overexpressed in prostate cancer cells and therefore is an attractive target for prostate cancer diagnosis and radionuclide therapy. Recently, published results from clinical studies using a new PSMA-targeting PET imaging agent, [ $^{68}\text{Ga}$ ]Ga-PSMA-093 ([ $^{68}\text{Ga}$ ]Ga-HBED-CC-O-carboxymethyl-Tyr-CO-NH-Glu), support the development of this agent for the diagnosis of prostate cancer. In this study, the HBED-CC chelating group in PSMA-093 was replaced by stereoselective (*R*)- or (*S*)-DOTAGA. This chelating group serves not only for chelating  $^{68}\text{Ga}$  but is also amendable for complexing other radioactive metals for radionuclide therapy. The corresponding optically pure (*R*)- and (*S*)-[ $^{68}\text{Ga}/^{177}\text{Lu}$ ]-DOTAGA derivatives, (*R*)-[ $^{68}\text{Ga}/^{177}\text{Lu}$ ]-13 and (*S*)-[ $^{68}\text{Ga}/^{177}\text{Lu}$ ]-13, were successfully prepared. Comparison of radiolabeling, binding affinity, cell uptake, and biodistribution between the two isomers was performed. Radiolabeling of (*R*)-[ $^{177}\text{Lu}$ ]Lu-13 and (*S*)-[ $^{177}\text{Lu}$ ]Lu-13 at 50 °C suggested that rates of complex formation were time-dependent and the formation of (*S*)-[ $^{177}\text{Lu}$ ]Lu-13 was distinctly faster. The rates of complex formation for the corresponding  $^{68}\text{Ga}$  agents were comparable between structural isomers. The  $^{\text{nat}}\text{Ga}$  and  $^{\text{nat}}\text{Lu}$  equivalents showed high binding PSMA affinity ( $\text{IC}_{50} = 24\text{--}111\text{ nM}$ ), comparable to that of the parent agent, [ $^{\text{nat}}\text{Ga}$ ]Ga-PSMA-093 ( $\text{IC}_{50} = 34.0\text{ nM}$ ). Results of cell uptake and biodistribution studies in PSMA-expressing PC3-PIP tumor-bearing mice appeared to show no difference between the labeled (*R*)- and (*S*)-isomers. This is the first time that a pair of [ $^{68}\text{Ga}/^{177}\text{Lu}$ ]-(*R*)- and (*S*)-DOTAGA isomers of PSMA agents were evaluated. Results of biological studies between the isomers showed no noticeable difference; however, the distinctions on the rate of Lu complex formation should be considered in the development of new  $^{177}\text{Lu}$ -DOTAGA-based radionuclide therapy agents in the future.

**KEYWORDS:** prostate cancer, gallium, lutetium, DOTAGA, chelating agents, optical isomers, PSMA, cell uptake, biodistribution

## INTRODUCTION

In the past few years,  $^{68}\text{Ge}/^{68}\text{Ga}$  generators have increasingly played an important role in nuclear medicine clinics.<sup>1,2</sup> It is known that  $^{68}\text{Ga}$  generator-based PET imaging agents have several unique advantages: (a) Germanium-68 ( $^{68}\text{Ge}$ ) ( $t_{1/2}$ , 271 days), a long-lived isotope, facilitates a widespread generator circulation; (b) physical properties of  $^{68}\text{Ga}$  ( $t_{1/2}$ , 68 min; 89%  $\beta^+$ ; 1.92 MeV max energy) are appropriate for PET imaging; (c)  $^{68}\text{Ge}/^{68}\text{Ga}$  generators provide an easy distribution for obtaining a positron-emitting isotope without the need of a nearby cyclotron.<sup>2,3</sup> For radionuclide therapy, decay characteristics of  $^{177}\text{Lu}$  ( $t_{1/2} = 6.71$  days,  $\beta^-$  (max) = 497 keV) are very attractive and they have been successfully applied in treatment of different cancers. Recently, Lu-177 DOTATATE (Lutathera) was approved by the FDA for the treatment of gastroenteropancreatic neuroendocrine tumors. This is the first time that a Lu-177 radiopharmaceutical has been approved for therapeutic application.<sup>4</sup> In addition, Lu-177 PSMA-617 is currently under clinical trials as a PSMA-targeting radionuclide therapy agent.<sup>5,6</sup>

A large number of Ga and Lu complexes have been reported, and they are usually based on macrocyclic or acyclic polyaza carboxylic acids as chelating groups, including DTPA, TRAP, AAZTA, DEDPA, DOTA, DOTAGA, and NOTAGA (see Figure 1 and Abbreviations). Many of these ligands are commonly employed to chelate radioactive metal ions including  $^{68}\text{Ga}(\text{III})$  and  $^{177}\text{Lu}(\text{III})$ .<sup>7</sup> Literature reports on DOTA and related ligands<sup>7,8</sup> suggest that they are the most versatile chelating agents forming Ga(III) and Lu(III) complexes with high thermodynamic stabilities. Nevertheless, the rate of complexation of no-carrier-added (n.c.a.)  $^{68}\text{Ga}$  and  $^{177}\text{Lu}$  with DOTA derivatives is relatively slow, thus requires heating at 80–



Received: July 26, 2020

Revised: October 13, 2020

Accepted: October 14, 2020

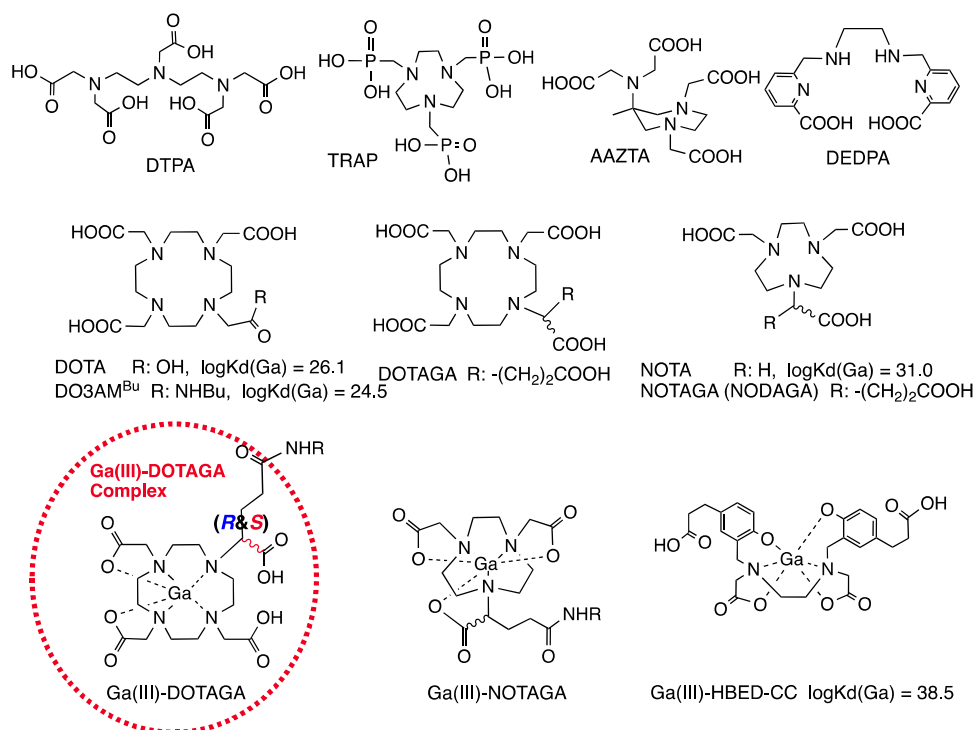


**Figure 1.** Various chelating agents commonly used for developing  $^{68}\text{Ga}$  and  $^{177}\text{Lu}$  imaging and radionuclide therapeutic agents. They include DTPA, TRAP, AAZTA, DEDPA, DOTA, DOTAGA, DOTA, and NOTAGA.<sup>7</sup>

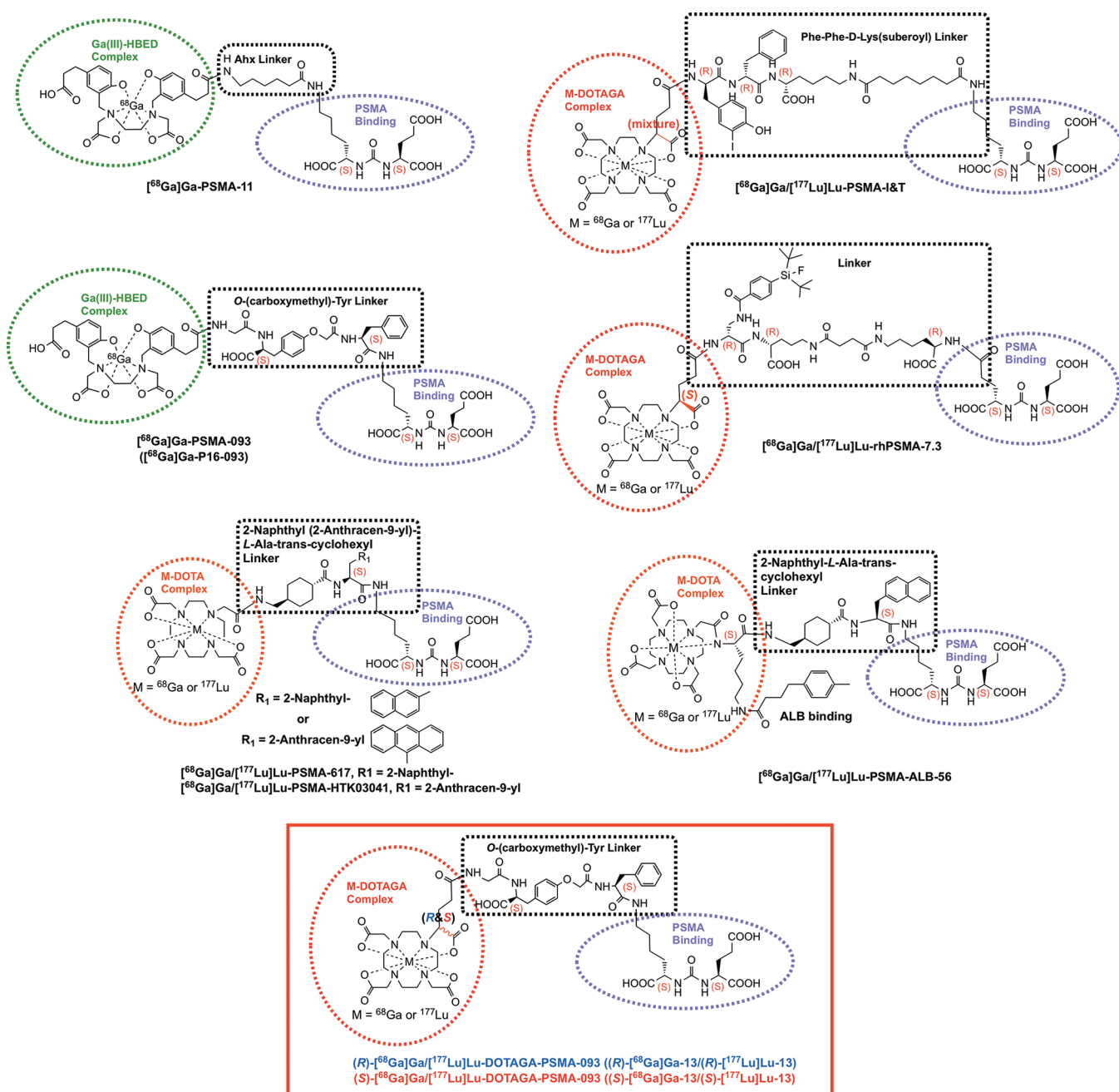
100 °C to complete the chelate formation. Generally, DOTA derivatives are prepared with one of the chelating carboxylic acid groups replaced by an amide substituted with additional groups; therefore, most of the time, they were designated as the DO3AM derivatives (Figure 1). It was reported that the kinetics and thermodynamic equilibrium constant of Ga-DO3AMBu ( $\log K_d = 24.6$ ) were less favorable than that of Ga-DOTA ( $\log K_d = 26.1$ ).<sup>9</sup> As Ga(III) has a relatively small ionic radius (187 pm), the complex formation between NOTA and Ga(III) is more rapid than that of DOTA or DO3AM derivatives. It is likely due to the fact that the smaller cavity created by NOTA derivatives is better adapted to the ionic radius of Ga(III) ( $\log K_d = 31.0$ ). The NOTAGA derivatives, containing an extra glutamic acid arm, form Ga-NOTAGA complexes that exhibit higher thermodynamic stability with faster complex formation kinetics. Complex formation of Ga(III) generally requires an octahedral coordination sphere, and Ga-NOTAGA analogues provide optimal in vitro and in vivo stability (Figure 1).<sup>10</sup>

Using a similar approach by adding one additional glutamic arm to DOTA, an alternative strategy in improving the kinetics of complex formation has been reported. Significantly, [ $^{68}\text{Ga}$ ]Ga-DOTAGA-TATE and [ $^{68}\text{Ga}$ ]Ga-DOTAGA-TOC showed improved  $^{68}\text{Ga}$  labeling and retained the biological binding affinity to the somatostatin receptors for imaging endocrine tumors.<sup>11</sup> However, there was no information provided on the optical purity of the complexing group DOTAGA; presumably, it was a racemic mixture. The interest of using DOTAGA for binding metal radionuclides does not stop at  $^{68}\text{Ga}$  imaging agents. The chelating agent is also known to complex many other useful radiometals, such as  $^{177}\text{Lu}$ ,  $^{44}\text{Sc}$ ,  $^{111}\text{In}$ ,  $^{89}\text{Zr}$ , and  $^{225}\text{Ac}$ .<sup>7,12</sup> Investigation on the effect of isomers introduced by the extra glutamic acid arm of DOTAGA ((R)- vs (S)-glutamic isomers) would be important for future develop-

ment of metal complexes for diagnosis and radionuclide therapy in personalized medicine.<sup>13</sup>

It is well-known that the HBED chelating group is not suitable for complexing Lu, and the cavity of DOTA derivatives is better suited for formation of Lu complexes.<sup>7</sup> By adding a glutamic acid arm, several  $^{68}\text{Ga}$ - and  $^{177}\text{Lu}$ -labeled DOTAGA derivatives designed for targeting PSMA binding were prepared and evaluated previously. Notably, [ $^{68}\text{Ga}$ ]Ga-DOTAGA-Phe-Phe-D-Lys(suberoyl)-Lys-urea-Glu and the related derivative PSMA-I&T<sup>14</sup> (see Figure 2) containing an extra glutamic acid arm provided enhanced  $^{68}\text{Ga}$  and  $^{177}\text{Lu}$  complex stability, and favorable pharmacokinetics and high specific binding to a PSMA tumor were described. This PSMA-ligand, [ $^{68}\text{Ga}/^{177}\text{Lu}$ ]Ga/Lu-PSMA-I&T, displayed potential for the management of prostate cancer.<sup>15,16</sup> However, the optical center of the glutamic acid arm for this agent was not specified, and it is assumed that racemic mixtures were used. These previous studies have demonstrated the “beneficial effect” of DOTAGA for DOTA substitution and using a (D)-amino acid ((R)-isomer) peptide linker on PSMA to improve affinity and metabolic stability for tumor uptake and clearance of nonspecific binding.<sup>14,15,17</sup>

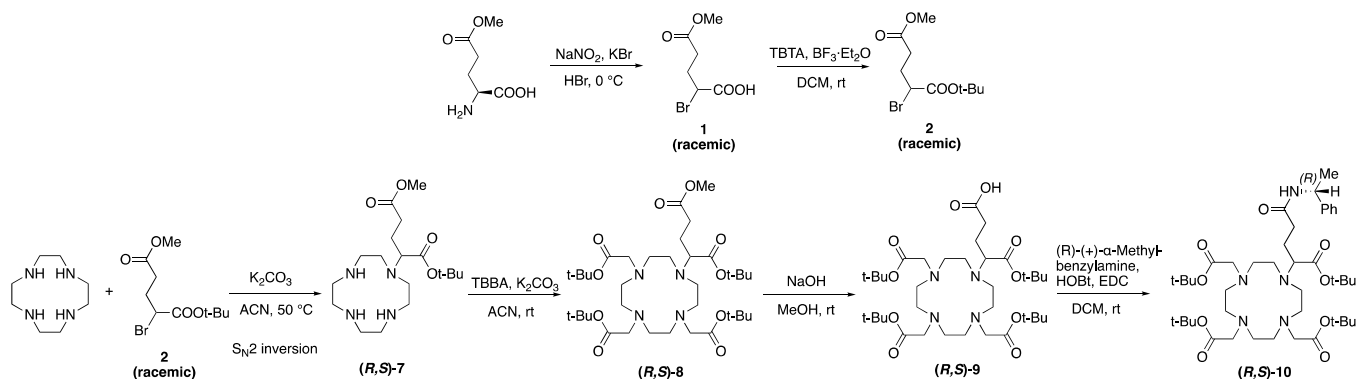
Recent reports on cancer statistics show that prostate cancer (PCa) is the second most common cancer diagnosed in men and fifth leading cause of cancer-related deaths worldwide.<sup>18,19</sup> PSMA is overexpressed in hormone-refractory and metastatic prostate cancer and is an excellent target for the diagnostic and therapeutic applications.<sup>20,21</sup> Many  $^{68}\text{Ga}$ -labeled PET imaging agents targeting PSMA expression for diagnosis of prostate cancer have been successfully tested clinically, including [ $^{68}\text{Ga}$ ]Ga-PSMA-11,<sup>2</sup> [ $^{68}\text{Ga}$ ]Ga-PSMA-THP,<sup>22</sup> [ $^{68}\text{Ga}$ ]Ga-PSMA-I&T,<sup>16</sup> [ $^{68}\text{Ga}$ ]Ga-PSMA-617,<sup>23,24</sup> and [ $^{68}\text{Ga}$ ]Ga-PSMA-093<sup>25</sup> (Figure 2). There are several advantages of using HBED instead of commonly employed DOTA and NOTA for chelating Ga(III). Stability constants ( $\log K_d$ ) for Ga-DOTA<sup>26</sup>



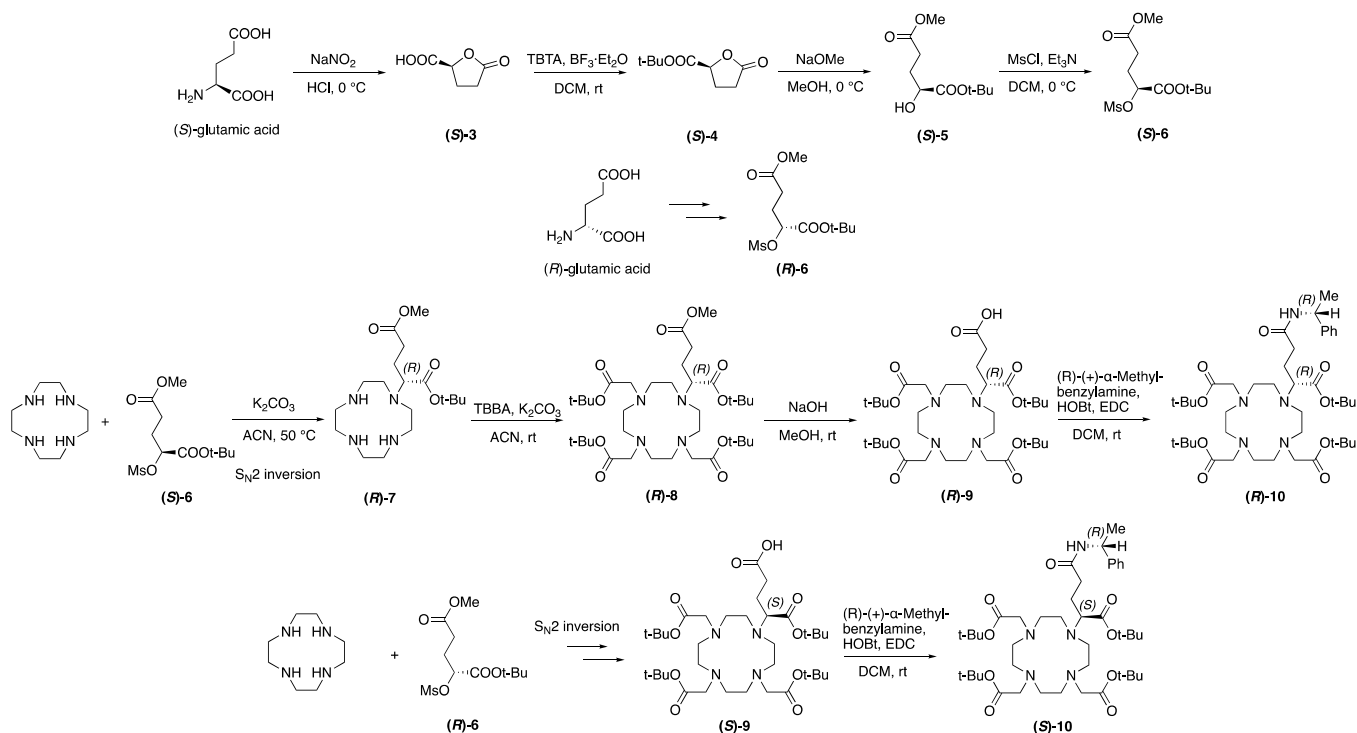
**Figure 2.** Chemical structures of several  $^{68}\text{Ga}/^{177}\text{Lu}$ -PSMA diagnostic imaging and radionuclide therapeutic agents. Each structure contains three parts (as indicated by colored spheres): (1) Ga/Lu complexing group: either HBED-CC (in green) or DOTA (in blue) or DOTAGA (in red) with an (R)- or (S)-optical center; (2) a linker (in black); and (3) a PSMA binding urea moiety,  $-\text{NH}-\text{CO}-\text{NH}-\text{Glu}$ , for PSMA binding (in purple). The new PSMA agents, (R)- and (S)-DOTAGA-PSMA-093, are marked by the solid red box. It is noted that the extra glutamic acid arm attached to the DOTAGA chelating group of rhPSMA-7.3,<sup>30–33</sup> a radiohybrid PSMA-targeting agent, is reported to be the (S)-isomer. The derivatives of [ $^{177}\text{Lu}$ ]Lu-PSMA-617, [ $^{177}\text{Lu}$ ]Lu-PSMA-HTK03041, and [ $^{177}\text{Lu}$ ]Lu-PSMA-ALB-56, which improved the in vivo pharmacokinetics, were recently reported in animal and clinical trials.<sup>34,35</sup>

and Ga-NOTA<sup>27</sup> complexes were previously reported ( $\log K_d = 21.3$  and  $31.0$ , respectively). Compared to DOTA and NOTA, the HBED chelating group forms a stronger, more stable Ga(III) complex: a  $\log K_d$  value of  $38.5$  was reported for Ga-HBED.<sup>7,28</sup> It is important to note that [ $^{177}\text{Lu}$ ]Lu-PSMA-617, a DOTA derivative, is currently the most well-studied PSMA-targeting radionuclide therapy agent. Clinical studies have clearly demonstrated its treatment potential in patients with metastatic castrate-resistant prostate cancer.<sup>5</sup>

Based on [ $^{68}\text{Ga}$ ]Ga-PSMA-11, a new PSMA-targeting agent [ $^{68}\text{Ga}$ ]Ga-PSMA-093 ([ $^{68}\text{Ga}$ ]Ga-P16-093), using a different linker, was developed (see Figure 2). Similarly, it is composed of three parts: [ $^{68}\text{Ga}$ ]Ga-HBED-CC complex (green circle), a novel linker *o*-(carboxymethyl)-L-tyrosine, and a PSMA binding group,  $-\text{Lys}-\text{NH}-\text{CO}-\text{NH}-\text{Glu}$  (purple circle) (see Figure 2).<sup>29</sup> The unique *o*-(carboxymethyl)-Tyr linker (black square box) of [ $^{68}\text{Ga}$ ]Ga-PSMA-093, as compared to the Ahx linker in [ $^{68}\text{Ga}$ ]Ga-PSMA-11, led to improvements on biological properties of PSMA targeting and lowering renal excretion. In vitro

Scheme 1. Synthesis of **2** and Diastereomers, *(R)*-(+)- $\alpha$ -Methylbenzylamide-DOTAGA(<sup>t</sup>Bu)<sub>4</sub> (*(R,S)*-10)<sup>a</sup>

<sup>a</sup>TBTA (*tert*-butyl trichloroacetimide) and TBBA (*tert*-butyl bromoacetate).

Scheme 2. Synthesis of *(S)*-6, *(R)*-6, and diastereomers, *(R)*-(+)- $\alpha$ -Methylbenzylamide-DOTAGA(<sup>t</sup>Bu)<sub>4</sub> (*(R)*-10 and *(S)*-10)

binding showed that [<sup>68</sup>Ga]Ga-PSMA-093 displayed fast labeling, excellent affinity (IC<sub>50</sub> = 33.5 nM), and specificity, a value comparable to that of [<sup>68</sup>Ga]Ga-PSMA-11.<sup>29</sup> Preliminary human studies (IND 133,222)<sup>25</sup> comparing PET images of [<sup>68</sup>Ga]Ga-PSMA-093 and [<sup>68</sup>Ga]Ga-PSMA-11 at 60 min after iv injection in the same prostate cancer patients showed similar ability to detect PSMA-positive prostate cancer. Furthermore, there are several notable advantages of [<sup>68</sup>Ga]Ga-PSMA-093 as compared to that of [<sup>68</sup>Ga]Ga-PSMA-11, including a lower renal clearance and minimum bladder activity while maintaining avid tumor uptake as compared to background.<sup>25</sup> Lower bladder uptake reduced background in the pelvic region, which has added advantage to visualize tumors in the prostate and regional lymph nodes. [<sup>68</sup>Ga]Ga-PSMA-093 appeared to be a promising candidate as a PET imaging radiotracer for detecting PSMA expression in prostate cancer.

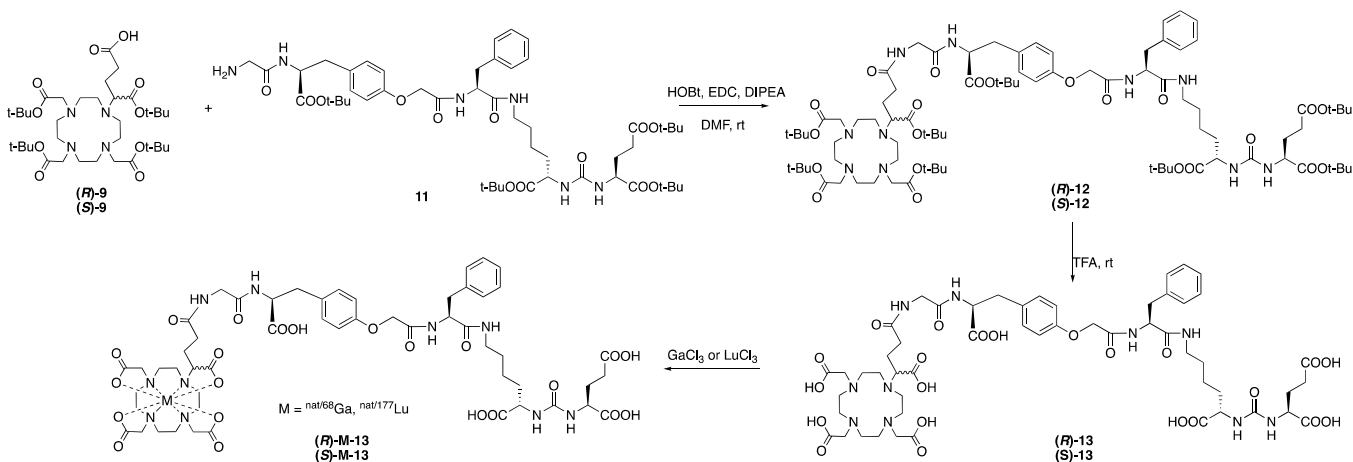
As mentioned above, HBED-CC is not suitable for complexing <sup>177</sup>Lu; in order to convert PSMA-093 for labeling with <sup>177</sup>Lu, the HBED-CC group was replaced by the *(R)*- or *(S)*-DOTAGA

chelating group (see red solid line box in Figure 2). It was hypothesized that using *(R)*- and *(S)*-DOTAGA derivatives, containing an extra glutamic acid arm on DOTA, could lead to development of new <sup>68</sup>Ga/<sup>177</sup>Lu-PSMA theragnostic agents. Both *(R)*- and *(S)*-DOTAGA isomers were expected to form stable complexes with <sup>177</sup>Lu.

Reported herein is the preparation, labeling, and biological evaluation of *(R)*- and *(S)*-DOTAGA-PSMA-093, (solid red box in Figure 2) as new PSMA-targeting agents for both diagnostic imaging (<sup>68</sup>Ga) and radionuclide therapy (<sup>177</sup>Lu). In particular, comparison of *(R)*- vs *(S)*-DOTAGA in <sup>68</sup>Ga and <sup>177</sup>Lu complex formation and potential effects of the optical center of the glutamic acid arm on PSMA-targeting properties were investigated.

## ■ MATERIALS AND METHODS

**General.** All reagents were commercial products used without further purification unless indicated. Solvents were

Scheme 3. Synthesis of (R)-[<sup>nat</sup>Ga]Ga-13, (R)-[<sup>nat</sup>Lu]Lu-13, (S)-[<sup>nat</sup>Ga]Ga-13, and (S)-[<sup>nat</sup>Lu]Lu-13<sup>a</sup>

<sup>a</sup>HOBt (hydroxybenzotriazole), EDC (1-(3-dimethylaminopropyl)-3-ethylcarbodiimide hydrochloride), and DIPEA (*N,N*-diisopropylethylamine).

dried through a molecular sieve system (Pure Solve Solvent Purification System; Innovative Technology, Inc.). <sup>1</sup>H NMR spectra were recorded on a Bruker Avance II spectrometer at 400 MHz and referenced to NMR solvents as indicated. High-resolution mass spectrometry (HRMS) data were obtained with an Agilent (Santa Clara, CA) G3250AA LC/MSD TOF system. Generally, crude compounds were purified by flash column chromatography (FC) packed with silica gel (Aldrich). A Wizard2 automatic gamma counter (PerkinElmer) measured <sup>68</sup>Ga and <sup>177</sup>Lu radioactivity. Reactions of nonradioactive chemical compounds were monitored by TLC analysis with precoated plates of silica gel 60 F254. Gallium-68 was obtained from a <sup>68</sup>Ge/<sup>68</sup>Ga generator (1.11 GBq (30 mCi)) produced by ITG (Isotope Technologies Garching GmbH). Lutetium-177 used in this research was supplied by the U.S. Department of Energy Isotope Program, managed by the Office of Science for Nuclear Physics.

**Chemistry.** The synthesis of (R)-13 and (S)-13 is outlined in Schemes 1–3. The details of the synthesis of 2 and (R)-6 are included in the Supporting Information.

**(S)-5-Oxotetrahydrofuran-2-carboxylic Acid ((S)-3).**<sup>36</sup> To a solution of (S)-glutamic acid (3.0 g, 20 mmol) in water (20 mL) was added hydrochloric acid (HCl, 37%, 5 mL) slowly at ice bath temperature. After being stirred at 0 °C for 20 min, a solution of sodium nitrite (2.1 g, 30 mmol) in water (5 mL) was added dropwise over 2 h at 0 °C. After completion of the addition, the reaction was warmed to rt and stirred overnight. The reaction mixture was extracted with ethyl acetate (EtOAc, 30 mL × 3). The combined organic layers were dried over magnesium sulfate (MgSO<sub>4</sub>) and filtered. The filtrate was concentrated and without further purification yielded 2.1 g of (S)-3 (yield, 80%) as a colorless oil. <sup>1</sup>H NMR (400 MHz, CDCl<sub>3</sub>): δ 5.01–4.98 (m, 1H), 2.72–2.52 (m, 3H), 2.46–2.36 (m, 1H).

**tert-Butyl (S)-5-Oxotetrahydrofuran-2-carboxylate ((S)-4).**<sup>36</sup> (S)-3 (1.6 g, 12.3 mmol) was dissolved in dichloromethane (CH<sub>2</sub>Cl<sub>2</sub>, 10 mL) in a 50 mL round-bottom flask. To this solution, *tert*-butyl 2,2,2-trichloroacetimidate (TBTA, 5.4 g, 25.0 mmol in 15 mL of cyclohexane) and boron trifluoride diethyl etherate (BF<sub>3</sub>·Et<sub>2</sub>O, 0.2 mL, 1.2 mmol) were added at 0 °C. After the addition was complete, the reaction mixture was warmed to rt and allowed to stir for 5 h. The reaction mixture was concentrated under reduced pressure, and the residue was

purified by FC (hexane/EtOAc = 70/30) to give 2.0 g of (S)-4 (yield, 87%) as a white solid. <sup>1</sup>H NMR (400 MHz, CDCl<sub>3</sub>): δ 4.81–4.78 (m, 1H), 2.65–2.44 (m, 3H), 2.28–2.23 (m, 1H), 1.48 (s, 9H).

**1-(tert-Butyl) 5-Methyl (S)-2-Hydroxypentanedioate ((S)-5).**<sup>37</sup> To a solution of (S)-4 (2.0 g, 10.7 mmol) in methanol (MeOH, 20 mL) was added sodium methoxide (0.6 g, 12.0 mmol) at 0 °C. After 30 min, the reaction was quenched with 1 M HCl and the mixture was concentrated under reduced pressure. Then, the residue was extracted with EtOAc (30 mL × 3). The combined organic layers were dried over MgSO<sub>4</sub> and filtered. The filtrate was purified by FC (hexane/EtOAc = 70/30) to give 1.8 g of (S)-5 (yield, 77%) as a colorless oil. <sup>1</sup>H NMR (400 MHz, CDCl<sub>3</sub>): δ 4.10–4.07 (m, 1H), 3.68 (s, 3H), 2.54–2.38 (m, 2H), 2.18–2.09 (m, 1H), 1.93–1.83 (m, 1H), 1.48 (s, 9H).

**1-(tert-Butyl) 5-Methyl (S)-2-((Methylsulfonyl)oxy)pentanedioate ((S)-6).**<sup>36</sup> To a solution of (S)-5 (1.4 g, 6.4 mmol) in dichloromethane (CH<sub>2</sub>Cl<sub>2</sub>, 30 mL) were added methanesulfonyl chloride (MsCl, 0.8 g, 7.0 mmol) and triethylamine (Et<sub>3</sub>N, 1.0 g, 9.6 mmol) dropwise at 0 °C. After completion of the addition, the reaction was warmed to rt and stirred for 1 h. Then, the reaction mixture was washed with brine (20 mL × 2) and water. The organic layers were dried over MgSO<sub>4</sub> and filtered. The filtrate was purified by FC (hexane/EtOAc = 70/30) to give 1.7 g of (S)-6 (yield, 90%) as a colorless oil. <sup>1</sup>H NMR (400 MHz, CDCl<sub>3</sub>): δ 4.99–4.96 (m, 1H), 3.70 (s, 3H), 3.14 (s, 3H), 2.52–2.48 (m, 2H), 2.34–2.25 (m, 1H), 2.19–2.10 (m, 1H), 1.50 (s, 9H). [ $\alpha$ ]<sub>D</sub><sup>25</sup> = –19.5 (MeOH, *c* = 2 mg/mL), [ $\alpha$ ]<sub>D</sub><sup>28</sup> = –16.0 (MeOH, *c* = 2 mg/mL).

**1-(tert-Butyl) 5-Methyl (R)-2-(1,4,7,10-Tetraazacyclododecan-1-yl)pentanedioate ((R)-7).** To a solution of 1,4,7,10-tetraazacyclododecane (344 mg, 2.0 mmol) in acetonitrile (ACN, 10 mL), K<sub>2</sub>CO<sub>3</sub> (137 mg, 1.0 mmol) was added at rt and stirred for 10 min. Then, (S)-6 (296 mg, 1.0 mmol) was dissolved in ACN (10 mL) and added dropwise. After completion of the addition, the reaction was warmed to 50 °C and stirred overnight. The reaction mixture was concentrated under reduced pressure, and the residue was purified by FC (CH<sub>2</sub>Cl<sub>2</sub>/MeOH/NH<sub>4</sub>OH = 80/20/2) to give 220 mg of (R)-7 (yield, 60%) as a colorless oil. <sup>1</sup>H NMR (400 MHz, CDCl<sub>3</sub>): δ 3.66 (s, 3H), 3.32–3.28 (m, 1H), 2.89–2.45 (m, 23H), 1.45 (s,

9H). HRMS: (M + H)<sup>+</sup> calcd for C<sub>18</sub>H<sub>37</sub>N<sub>4</sub>O<sub>4</sub>, 373.2815; found, 373.2846.

**1-(tert-Butyl) 5-Methyl (S)-2-(1,4,7,10-Tetraazacyclododecan-1-yl)pentanedioate ((S)-7).** Compound (S)-7 (350 mg; yield, 60%) was prepared from (R)-6 (466 mg, 1.57 mmol), 1,4,7,10-tetraazacyclododecane (516 mg, 3.1 mmol), and K<sub>2</sub>CO<sub>3</sub> (215 mg, 1.57 mmol) following the same procedure as for (R)-7 as a colorless oil. <sup>1</sup>H NMR (400 MHz, CDCl<sub>3</sub>): δ 3.68 (s, 3H), 3.32–3.22 (m, 1H), 2.92–2.44 (m, 23H), 1.46 (s, 9H). HRMS: (M + H)<sup>+</sup> calcd for C<sub>18</sub>H<sub>37</sub>N<sub>4</sub>O<sub>4</sub>, 373.2815; found, 373.2839.

**1-(tert-Butyl) 5-Methyl 2-(1,4,7,10-Tetraazacyclododecan-1-yl)pentanedioate ((R,S)-7).** Compound (R,S)-7 (200 mg; yield, 53%) was prepared from 2 (280 mg, 1.0 mmol), 1,4,7,10-tetraazacyclododecane (344 mg, 2.0 mmol), and K<sub>2</sub>CO<sub>3</sub> (137 mg, 1.0 mmol) following the same procedure as for (R)-7 as a colorless oil. <sup>1</sup>H NMR (400 MHz, CDCl<sub>3</sub>): δ 3.66 (s, 3H), 3.31–3.28 (m, 1H), 2.88–2.44 (m, 23H), 1.45 (s, 9H). HRMS: (M + H)<sup>+</sup> calcd for C<sub>18</sub>H<sub>37</sub>N<sub>4</sub>O<sub>4</sub>, 373.2815; found, 373.2842.

**1-(tert-Butyl) 5-Methyl (R)-2-(4,7,10-Tris(2-(tert-butoxy)-2-oxoethyl)-1,4,7,10-tetraazacyclododecan-1-yl)pentanedioate ((R)-8).** To a solution of (R)-7 (60 mg, 0.16 mmol) in ACN (10 mL), K<sub>2</sub>CO<sub>3</sub> (137 mg, 1.0 mmol) and *tert*-butyl bromoacetate (TBBA, 136 mg, 0.7 mmol) were added at 0 °C. The reaction mixture was warmed to rt and stirred overnight. Then, the reaction mixture was concentrated under reduced pressure and the residue was purified by FC (CH<sub>2</sub>Cl<sub>2</sub>/MeOH/NH<sub>4</sub>OH = 90/9/1) to give 70 mg of (R)-8 (yield, 60%) as a colorless oil. <sup>1</sup>H NMR (400 MHz, CDCl<sub>3</sub>): δ 3.60 (s, 3H), 3.41–3.15 (m, 7H), 2.97–2.31 (m, 16H), 2.27–1.81 (m, 4H), 1.45–1.40 (m, 36H). HRMS: (M + H)<sup>+</sup> C<sub>36</sub>H<sub>67</sub>N<sub>4</sub>O<sub>10</sub>, 715.4875; found, 715.4828.

**1-(tert-Butyl) 5-Methyl (S)-2-(4,7,10-Tris(2-(tert-butoxy)-2-oxoethyl)-1,4,7,10-tetraazacyclododecan-1-yl)pentanedioate ((S)-8).** Compound (S)-8 (212 mg; yield, 55%) was prepared from (S)-7 (200 mg, 0.54 mmol), TBBA (421 mg, 2.16 mmol), and K<sub>2</sub>CO<sub>3</sub> (444 mg, 3.24 mmol) following the same procedure as for (R)-8 as a colorless oil. <sup>1</sup>H NMR (400 MHz, CDCl<sub>3</sub>): δ 3.65 (s, 3H), 3.51–3.49 (m, 1H), 3.42–3.20 (m, 6H), 2.87–2.79 (m, 4H), 2.60–2.36 (m, 12H), 2.17–2.12 (m, 3H), 2.05–1.97 (m, 1H), 1.47 (s, 9H), 1.43–1.45 (m, 27H). HRMS: (M + H)<sup>+</sup> calcd for C<sub>36</sub>H<sub>67</sub>N<sub>4</sub>O<sub>10</sub>, 715.4875; found, 715.4793.

**1-(tert-Butyl) 5-Methyl 2-(4,7,10-Tris(2-(tert-butoxy)-2-oxoethyl)-1,4,7,10-tetraazacyclododecan-1-yl)pentanedioate ((R,S)-8).** Compound (R,S)-8 (200 mg; yield, 52%) was prepared from (R,S)-7 (200 mg, 0.54 mmol), TBBA (409 mg, 2.10 mmol), and K<sub>2</sub>CO<sub>3</sub> (438 mg, 3.20 mmol) following the same procedure as for (R)-8 as a colorless oil. <sup>1</sup>H NMR (400 MHz, CDCl<sub>3</sub>): δ 3.64–3.63 (m, 3H), 3.49–3.18 (m, 7H), 2.95–2.77 (m, 8H), 2.59–2.33 (m, 8H), 2.14–1.80 (m, 4H), 1.45–1.42 (m, 36H). HRMS: (M + H)<sup>+</sup> calcd for C<sub>36</sub>H<sub>67</sub>N<sub>4</sub>O<sub>10</sub>, 715.4875; found, 715.4811.

**(R)-5-(tert-Butoxy)-5-oxo-4-(4,7,10-tris(2-(tert-butoxy)-2-oxoethyl)-1,4,7,10-tetraazacyclododecan-1-yl)pentanoic Acid ((R)-9).** To a solution of (R)-8 (70 mg, 0.1 mmol) in methanol (5 mL) was added sodium hydroxide (NaOH, 1 N, 2 mL) dropwise. After being stirred at rt for 2 h, HCl (1 N) was added dropwise into the reaction mixture at 0 °C and adjusted the pH to 5–6. Then, the reaction mixture was concentrated under reduced pressure and the residue was purified by FC (CH<sub>2</sub>Cl<sub>2</sub>/MeOH/NH<sub>4</sub>OH = 90/9/1) to give 52 mg of (R)-9 (yield, 75%) as a colorless oil. <sup>1</sup>H NMR (400 MHz, CDCl<sub>3</sub>): δ

3.55–3.53 (m, 1H), 3.43–3.30 (m, 3H), 3.06–2.98 (m, 3H), 2.85–2.79 (m, 4H), 2.74–2.71 (m, 3H), 2.65–2.50 (m, 5H), 2.31–2.25 (m, 4H), 2.11–1.98 (m, 4H), 1.45 (s, 9H), 1.43–1.42 (m, 27H). HRMS: (M + H)<sup>+</sup> calcd for C<sub>35</sub>H<sub>65</sub>N<sub>4</sub>O<sub>10</sub>, 701.4701; found, 701.4770.

**(S)-5-(tert-Butoxy)-5-oxo-4-(4,7,10-tris(2-(tert-butoxy)-2-oxoethyl)-1,4,7,10-tetraazacyclododecan-1-yl)pentanoic Acid ((S)-9).** Compound (S)-9 (145 mg; yield, 70%) was prepared from (S)-8 (212 mg, 0.29 mmol) following the same procedure as for (R)-9 as a colorless oil. <sup>1</sup>H NMR (400 MHz, CDCl<sub>3</sub>): δ 3.63–3.61 (m, 1H), 3.51–3.47 (m, 1H), 3.41–3.28 (m, 2H), 2.94–2.73 (m, 7H), 2.66–2.57 (m, 8H), 2.45–2.34 (m, 2H), 2.25–2.17 (m, 3H), 2.08–2.04 (m, 3H), 1.44–1.46 (m, 36H). HRMS: (M + H)<sup>+</sup> calcd for C<sub>35</sub>H<sub>65</sub>N<sub>4</sub>O<sub>10</sub>, 701.4701; found, 701.4679.

**(R,S)-5-(tert-Butoxy)-5-oxo-4-(4,7,10-tris(2-(tert-butoxy)-2-oxoethyl)-1,4,7,10-tetraazacyclododecan-1-yl)pentanoic Acid ((R,S)-9).** Compound (R,S)-9 (156 mg; yield, 70%) was prepared from (R,S)-8 (200 mg, 0.28 mmol) following the same procedure as for (R)-9 as a colorless oil. <sup>1</sup>H NMR (400 MHz, CDCl<sub>3</sub>): δ 3.65–3.63 (m, 1H), 3.52–3.28 (m, 3H), 2.95–2.73 (m, 8H), 2.67–2.52 (m, 5H), 2.47–2.41 (m, 2H), 2.31–2.23 (m, 4H), 2.08–2.01 (m, 4H), 1.44–1.46 (m, 36H). HRMS: (M + H)<sup>+</sup> calcd for C<sub>35</sub>H<sub>65</sub>N<sub>4</sub>O<sub>10</sub>, 701.4701; found, 701.4677.

**Tri-tert-butyl 2,2',2''-(10-((R)-1-(tert-Butoxy)-1,5-dioxo-5-(((R)-1-phenylethyl)amino)pentan-2-yl)-1,4,7,10-tetraazacyclododecane-1,4,7-triyl)triacetate ((R)-10).** To a solution of (R)-9 (30 mg, 0.04 mmol) in CH<sub>2</sub>Cl<sub>2</sub> (5 mL) were added (R)-(+)- $\alpha$ -methylbenzylamine (8 mg, 0.06 mmol), hydroxybenzotriazole (HOBt, 8 mg, 0.06 mmol), and 1-(3-dimethylamino-propyl)-3-ethylcarbodiimide hydrochloride (EDC, 12 mg, 0.06 mmol) at 0 °C. The reaction mixture was stirred for 1 h before it was concentrated under reduced pressure. Then, the residue was purified by FC (CH<sub>2</sub>Cl<sub>2</sub>/MeOH/NH<sub>4</sub>OH = 90/9/1) to give 25 mg of (R)-10 (yield, 72%) as a colorless oil. <sup>1</sup>H NMR (400 MHz, CDCl<sub>3</sub>): δ 8.07 (d, J = 8.0 Hz, 1H), 7.49–7.47 (m, 2H), 7.30–7.26 (m, 2H), 7.19–7.15 (m, 1H), 5.08–5.04 (m, 1H), 3.53–3.31 (m, 4H), 2.99–2.48 (m, 15H), 2.27–1.90 (m, 8H), 1.55 (d, J = 7.2 Hz, 3H), 1.46–1.43 (m, 36H). HRMS: (M + H)<sup>+</sup> calcd for C<sub>43</sub>H<sub>74</sub>N<sub>5</sub>O<sub>9</sub>, 804.5487; found, 804.5510. [ $\alpha$ ]<sub>D</sub><sup>25</sup> = –79.0 (MeOH, c = 1 mg/mL). The optical purity of compound was analyzed by HPLC with a PRP-1 10  $\mu$ m, 250  $\times$  4.6 mm column. The (R)-10 was eluted under isocratic conditions (ACN/0.5% TFA in water (4/6), a flow rate of 2 mL/min, temperature-controlled column compartment set at 10 °C), and the retention time was 16.5 min.

**Tri-tert-butyl 2,2',2''-(10-((S)-1-(tert-Butoxy)-1,5-dioxo-5-(((R)-1-phenylethyl)amino)pentan-2-yl)-1,4,7,10-tetraazacyclododecane-1,4,7-triyl)triacetate ((S)-10).** Compound (S)-10 (30 mg; yield, 52%) was prepared from (S)-9 (50 mg, 0.07 mmol), (R)-(+)- $\alpha$ -methylbenzylamine (12 mg, 0.1 mmol), HOBt (13 mg, 0.1 mmol), and EDC (19 mg, 0.1 mmol) following the same procedure as for (R)-10 as a colorless oil. <sup>1</sup>H NMR (400 MHz, CDCl<sub>3</sub>): δ 8.63 (d, J = 8.0 Hz, 1H), 7.50–7.49 (m, 2H), 7.28–7.24 (m, 2H), 7.17–7.13 (m, 1H), 5.05–5.01 (m, 1H), 3.55–3.29 (m, 4H), 2.97–2.43 (m, 15H), 2.25–1.92 (m, 8H), 1.54 (d, J = 6.8 Hz, 3H), 1.46–1.45 (m, 36H). HRMS: (M + H)<sup>+</sup> calcd for C<sub>43</sub>H<sub>74</sub>N<sub>5</sub>O<sub>9</sub>, 804.5487; found, 804.5507. [ $\alpha$ ]<sub>D</sub><sup>25</sup> = +93.0 (MeOH, c = 1 mg/mL). (S)-10 was eluted under isocratic conditions (ACN/0.5% TFA in water (4/6), a flow rate of 2 mL/min, temperature-controlled column compartment set at 10 °C), and the retention time was 18.8 min.

*Tri-tert-butyl 2,2',2''-(10-(1-(tert-Butoxy)-1,5-dioxo-5-(((R)-1-phenylethylamino)pentan-2-yl)-1,4,7,10-tetraazacyclododecane-1,4,7-triyl)triacetate ((R,S)-10)*. Compound (R,S)-10 (20 mg; yield, 59%) was prepared from (R,S)-9 (30 mg, 0.04 mmol), (R)-(+)- $\alpha$ -methylbenzylamine (8 mg, 0.06 mmol), HOBT (8 mg, 0.06 mmol), and EDC (12 mg, 0.06 mmol) following the same procedure as for (R)-10 as a colorless oil.  $^1\text{H}$  NMR (400 MHz,  $\text{CDCl}_3$ ):  $\delta$  8.84–8.82 (m, 0.3H), 8.74–8.72 (m, 0.7H), 7.48–7.45 (m, 2H), 7.27–7.24 (m, 2H), 7.17–7.10 (m, 1H), 5.07–5.03 (m, 1H), 3.50–3.24 (m, 4H), 2.94–2.31 (m, 15H), 2.23–1.91 (m, 8H), 1.53–1.51 (m, 3H), 1.46–1.45 (m, 36H). HRMS:  $(\text{M} + \text{H})^+$  calcd for  $\text{C}_{43}\text{H}_{74}\text{N}_5\text{O}_9$ , 804.5487; found, 804.5493. (R,S)-10 was eluted under isocratic conditions (ACN/0.5% TFA in water (4/6), a flow rate of 2 mL/min, temperature-controlled column compartment set at 10 °C) with a ratio of (R)-10/(S)-10 7/3.

*Di-tert-butyl (((S)-1-(tert-Butoxy)-6-((S)-2-(2-(4-((S)-3-(tert-butoxy)-2-((R)-5-(tert-butoxy)-5-oxo-4-(4,7,10-tris(2-(tert-butoxy)-2-oxoethyl)-1,4,7,10-tetraazacyclododecan-1-yl)pentanamido)acetamido)-3-oxopropyl)phenoxy)acetamido)-3-phenylpropanamido)-1-oxohexan-2-yl)-carbamoyl)-L-glutamate ((R)-12)*. To a solution of (R)-9 (22 mg, 0.03 mmol) in *N,N*-dimethylformamide (DMF, 5 mL), *N,N*-diisopropylethylamine (DIPEA, 13 mg, 0.1 mmol), HOBT (7 mg, 0.05 mmol), EDC (9.5 mg, 0.05 mmol), and 11 (30 mg, 0.03 mmol) were added at 0 °C. The mixture was stirred at rt overnight before 20 mL of EtOAc was added to the reaction mixture. It was then washed with  $\text{H}_2\text{O}$  (10 mL  $\times$  2) and brine (10 mL), dried over  $\text{MgSO}_4$ , and filtered. The filtrate was concentrated, and the residue was purified by FC (DCM/MeOH/ $\text{NH}_4\text{OH}$  = 90/9/1) to give 40 mg of (R)-12 (yield, 78%) as a colorless oil.  $^1\text{H}$  NMR (400 MHz,  $\text{CDCl}_3$ ):  $\delta$  8.52 (t,  $J$  = 5.9 Hz, 1H), 7.68 (d,  $J$  = 8.8 Hz, 1H), 7.32–7.15 (m, 1H), 7.11 (d,  $J$  = 8.4 Hz, 2H), 6.77 (d,  $J$  = 8.4 Hz, 2H), 6.16 (d,  $J$  = 9.1 Hz, 1H), 5.99 (d,  $J$  = 7.9 Hz, 1H), 4.76 (d,  $J$  = 6.9 Hz, 1H), 4.61 (d,  $J$  = 7.1 Hz, 1H), 4.35–4.19 (m, 2H), 4.03 (dd,  $J$  = 16.7, 6.6 Hz, 1H), 3.75 (dd,  $J$  = 16.8, 5.2 Hz, 1H), 3.68–3.54 (m, 2H), 3.51–3.20 (m, 4H), 3.18–2.90 (m, 8H), 2.87–2.70 (m, 6H), 2.70–2.46 (m, 6H), 2.46–2.14 (m, 6H), 2.09–2.06 (m, 4H), 1.88–1.58 (m, 4H), 1.50–1.33 (m, 72H). HRMS:  $(\text{M} + \text{H})^+$  calcd for  $\text{C}_{85}\text{H}_{139}\text{N}_{10}\text{O}_{22}$ , 1652.0065; found, 1652.0026.

*Di-tert-butyl (((S)-1-(tert-Butoxy)-6-((S)-2-(2-(4-((S)-3-(tert-butoxy)-2-((S)-5-(tert-butoxy)-5-oxo-4-(4,7,10-tris(2-(tert-butoxy)-2-oxoethyl)-1,4,7,10-tetraazacyclododecan-1-yl)pentanamido)acetamido)-3-oxopropyl)phenoxy)acetamido)-3-phenylpropanamido)-1-oxohexan-2-yl)-carbamoyl)-L-glutamate ((S)-12)*. Compound (S)-12 (60 mg; yield, 51%) was prepared from (S)-9 (50 mg, 0.07 mmol), *N,N*-diisopropylethylamine (DIPEA, 25 mg, 0.2 mmol), HOBT (14 mg, 0.09 mmol), EDC (20 mg, 0.1 mmol), and 11 (70 mg, 0.07 mmol) following the same procedure as for (R)-12 as a colorless oil.  $^1\text{H}$  NMR (400 MHz,  $\text{CDCl}_3$ ):  $\delta$  8.64 (t,  $J$  = 5.6 Hz, 1H), 7.85 (d,  $J$  = 8.5 Hz, 1H), 7.56 (s, 1H), 7.37 (d,  $J$  = 7.4 Hz, 1H), 7.05 (d,  $J$  = 8.5 Hz, 2H), 6.67 (d,  $J$  = 8.5 Hz, 2H), 6.35 (d,  $J$  = 7.4 Hz, 1H), 6.12 (d,  $J$  = 7.8 Hz, 1H), 4.84–4.79 (m, 1H), 4.57–4.52 (m, 1H), 4.39–4.29 (m, 2H), 4.23–4.18 (m, 1H), 4.02–3.96 (m, 1H), 3.83–3.77 (m, 1H), 3.35–2.92 (m, 13H), 2.79–2.47 (m, 12H), 2.30–2.27 (m, 3H), 2.22–2.16 (m, 3H), 2.05–2.00 (m, 4H), 1.82–1.77 (m, 2H), 1.66–1.59 (m, 2H), 1.43–1.38 (m, 63H), 1.31 (s, 9H). HRMS:  $(\text{M} + \text{H})^+$  calcd for  $\text{C}_{85}\text{H}_{139}\text{N}_{10}\text{O}_{22}$ , 1652.0065; found, 1652.0078.

*(((S)-1-Carboxy-5-((S)-2-(2-(4-((S)-2-carboxy-2-((R)-4-carboxy-4-(4,7,10-tris(carboxymethyl)-1,4,7,10-tetraazacy-*

*clododecan-1-yl)butanamido)acetamido)ethyl)phenoxy)acetamido)-3-phenylpropanamido)pentyl)carbamoyl)-L-glutamic Acid ((R)-13)*. A solution of (R)-12 (40 mg, 0.024 mmol) in 1 mL of TFA was stirred at rt for 5 h. The reaction mixture was evaporated in vacuo. The residue was dissolved in 1 mL of DMSO and purified by semipreparative HPLC (Luna 10u C8(2) 250  $\times$  10.00 mm, ACN/0.1% TFA in water = 65/35, 4 mL/min) to give 15.5 mg of (R)-13 (yield, 54%) as a colorless oil.  $^1\text{H}$  NMR (400 MHz, DMSO):  $\delta$  8.18 (d,  $J$  = 6.9 Hz, 1H), 8.06 (d,  $J$  = 8.0 Hz, 1H), 7.21 (dd,  $J$  = 19.1, 9.0 Hz, 2H), 7.10 (d,  $J$  = 5.5 Hz, 1H), 6.97 (s, 1H), 6.74 (d,  $J$  = 8.6 Hz, 1H), 6.36–6.26 (m, 1H), 4.56–4.51 (m, 1H), 4.41–4.37 (m, 2H), 4.11–4.03 (m, 1H), 3.77–3.58 (m, 4H), 3.34–2.86 (m, 25H), 2.33–2.22 (m, 3H), 1.92–1.15 (m, 10H). HRMS:  $(\text{M} + \text{H})^+$  calcd for  $\text{C}_{53}\text{H}_{75}\text{N}_{10}\text{O}_{22}$ , 1203.5057; found, 1203.5104. (The LC–MS profile is shown in Figure S4.)

*(((S)-1-Carboxy-5-((S)-2-(2-(4-((S)-2-carboxy-2-((S)-4-carboxy-4-(4,7,10-tris(carboxymethyl)-1,4,7,10-tetraazacyclododecan-1-yl)butanamido)acetamido)ethyl)phenoxy)acetamido)-3-phenylpropanamido)pentyl)carbamoyl)-L-glutamic Acid ((S)-13)*. Compound (S)-13 (15.1 mg; yield, 41%) was prepared from (S)-12 (50 mg, 0.03 mmol) following the same procedure as for (R)-13 described above as a colorless oil.  $^1\text{H}$  NMR (400 MHz, DMSO):  $\delta$  8.18 (d,  $J$  = 6.9 Hz, 1H), 8.06 (d,  $J$  = 8.0 Hz, 1H), 7.21 (dd,  $J$  = 19.1, 9.0 Hz, 2H), 7.10 (d,  $J$  = 5.5 Hz, 1H), 6.97–6.95 (m, 1H), 6.74 (d,  $J$  = 8.6 Hz, 1H), 6.33–6.28 (m, 1H), 4.56–4.51 (m, 1H), 4.40–4.42 (m, 2H), 4.13–4.03 (m, 1H), 3.77–3.58 (m, 4H), 3.37–2.82 (m, 25H), 2.67–2.21 (m, 3H), 1.93–1.23 (m, 10H). HRMS:  $(\text{M} + \text{H})^+$  calcd for  $\text{C}_{53}\text{H}_{75}\text{N}_{10}\text{O}_{22}$ , 1203.5057; found, 1203.5094. (The LC–MS profile is shown in Figure S5.)

*(R)-[ $^{nat}\text{Ga}$ ]Ga-13*. (R)-13 (1 mg, 0.83  $\mu\text{mol}$ ) was dissolved in 254  $\mu\text{L}$  of dimethyl sulfoxide (DMSO) in a small vial, and 0.8  $\mu\text{L}$  of  $\text{GaCl}_3$  aqueous (1.14 M, 0.91  $\mu\text{mol}$ ) was added. The mixture was carefully adjusted by dropwise addition of 5  $\mu\text{L}$  of sodium acetate ( $\text{NaOAc}$ , 1 N) to pH = 4 and diluted with water to a final volume of 1 mL (1 mg/mL solution). The vial was closed, and the reaction mixture was stirred overnight at rt. The completion of the formation of (R)-[ $^{nat}\text{Ga}$ ]Ga-13 was verified by LC–MS where no (R)-13 could be anymore detected. The resulting aqueous solution (1 mg/mL (R)-[ $^{nat}\text{Ga}$ ]Ga-13) was diluted and used in the in vitro binding affinity studies without further processing. HRMS:  $(\text{M} + \text{H})^+$  calcd for  $\text{C}_{53}\text{H}_{72}\text{N}_{10}\text{O}_{22}\text{Ga}$ , 1269.4078; found, 1269.4053. (The LC–MS profile is shown in Figure S6.)

*(S)-[ $^{nat}\text{Ga}$ ]Ga-13*. (S)-[ $^{nat}\text{Ga}$ ]Ga-13 was prepared from (S)-13 (1 mg, 0.83  $\mu\text{mol}$ ) following the same procedure as for (R)-[ $^{nat}\text{Ga}$ ]Ga-13. HRMS:  $(\text{M})^+$  calcd for  $\text{C}_{53}\text{H}_{72}\text{N}_{10}\text{O}_{22}\text{Ga}$ , 1269.4078; found, 1269.4070. (The LC–MS profile is shown in Figure S7.)

*(R)-[ $^{nat}\text{Lu}$ ]Lu-13*. (R)-13 (1 mg, 0.83  $\mu\text{mol}$ ) was dissolved in 254  $\mu\text{L}$  of DMSO in a small vial, and 9  $\mu\text{L}$  of  $\text{LuCl}_3$  aqueous (30 mg/mL, 0.91  $\mu\text{mol}$ ) was added. The mixture was carefully adjusted by dropwise addition of 10  $\mu\text{L}$  of  $\text{NaOAc}$  (1 N) to pH = 5 and diluted with water to a final volume of 1 mL (1 mg/mL solution). The vial was closed, and the reaction mixture was stirred for 2 h at 90 °C. The completion of the formation of (R)-[ $^{nat}\text{Lu}$ ]Lu-13 was verified by LC–MS where no (R)-13 could be anymore detected. The resulting aqueous solution (1 mg/mL (R)-[ $^{nat}\text{Lu}$ ]Lu-13) was further diluted and used in in vitro binding affinity studies without further processing. HRMS:  $(\text{M} + \text{H})^+$  calcd for  $\text{C}_{53}\text{H}_{70}\text{N}_{10}\text{O}_{22}\text{Lu}$ , 1375.4230; found, 1375.4173. (The LC–MS profile is shown in Figure S8.)

(*S*)-[<sup>nat</sup>Lu]Lu-13. (*S*)-[<sup>nat</sup>Lu]Lu-13 was prepared from (*S*)-13 (1 mg, 0.83 μmol) following the same procedure as for (*R*)-[<sup>nat</sup>Lu]Lu-13. HRMS: (M + H)<sup>+</sup> calcd for C<sub>53</sub>H<sub>70</sub>N<sub>10</sub>O<sub>22</sub>Lu, 1375.4230; found, 1375.4203. (The LC–MS profile is shown in Figure S9.)

**Comparison of Radiolabeling of (*R*)- and (*S*)-[<sup>68</sup>Ga]Ga-13 and (*R*)- and (*S*)-[<sup>177</sup>Lu]Lu-13 to [<sup>68</sup>Ga]Ga-PSMA-617 and [<sup>177</sup>Lu]Lu-PSMA-617.** Eluent <sup>68</sup>GaCl<sub>3</sub> (0.3 mL) in 0.05 M HCl from a <sup>68</sup>Ge/<sup>68</sup>Ga generator and 30 μL of 0.5 N NaOAc were mixed and added to 5 μg of (*R*)- and (*S*)-13 or PSMA-617 (in DMSO). <sup>177</sup>LuCl<sub>3</sub> (10 μL, 1.85 MBq, ≤925 GBq/mg, in 0.05 M HCl (0.43 mL)) and 50 μL of 0.5 N NaOAc were mixed and added to 2 μg of (*R*)- and (*S*)-13 or PSMA-617 (in DMSO). The reaction mixtures were incubated at 50 °C, and aliquots were removed at different time points (5, 10, 15, 20, 25, and 30 min). The radiochemical yields were determined by TLC (iTLC-SG CH<sub>3</sub>OH, H<sub>2</sub>O, 30% NH<sub>4</sub>OH (2:2:0.1 v/v/v)).

**Comparison of Radiolabeling of (*R*)- and (*S*)-[<sup>68</sup>Ga]Ga-13, (*R*)- and (*S*)-[<sup>177</sup>Lu]Lu-13, and [<sup>177</sup>Lu]Lu-PSMA-617 for In Vitro and In Vivo Studies.** <sup>68</sup>GaCl<sub>3</sub> (0.5 mL, 55.5 MBq) in 0.05 M HCl of a <sup>68</sup>Ge/<sup>68</sup>Ga generator and 50 μL of 0.5 N NaOAc were mixed and added to 20 μg of (*R*)- and (*S*)-13 (in DMSO). The reaction mixture was incubated at 80 °C for 10 min. [<sup>68</sup>Ga]Ga-PSMA-093 was synthesized following the reported method.<sup>29</sup> <sup>177</sup>LuCl<sub>3</sub> (10 μL, 18.5 MBq, ≤925 GBq/mg) was diluted with 0.05 M HCl (0.43 mL), and 50 μL of 0.5 N NaOAc was added and mixed with 10 μg of (*R*)- and (*S*)-13 or PSMA-617 (in DMSO). The reaction mixtures were incubated at 80 °C for 20 min. Radiochemical yields were determined by radio-HPLC (stationary phase: Supelco Ascentis C18, 5 μm, 150 × 4.6 mm) column; mobile phase: 0.1% TFA in water/ACN with a gradient of 0–15 min, from 100% H<sub>2</sub>O with 0.1% TFA to 100% ACN; and a flow rate of 1 mL/min). Radiochemical purities of all [<sup>68</sup>Ga]Ga-labeled and [<sup>177</sup>Lu]Lu-labeled agents, (*R*)- and (*S*)-[<sup>68</sup>Ga]Ga-13 (30 μM, 1.6 GBq/μmol), (*R*)- and (*S*)-[<sup>177</sup>Lu]Lu-13 (16 μM, 2.3 GBq/μmol), and [<sup>177</sup>Lu]Lu-PSMA617, were >95%. The tracers were diluted and used in vitro and in vivo experiments without purification.

**In Vitro Stability in PBS and Plasma.** (*R*)- and (*S*)-[<sup>177</sup>Lu]Lu-13 were synthesized in 20 min at 80 °C as described above. These tracers (RCPs, >95%) were used for in vitro stability without purification. (*R*)- and (*S*)-[<sup>177</sup>Lu]Lu-13 were added to 0.1 M phosphate-buffered saline (PBS, pH 7.0) or plasma (purchased from Innovative Research, MI), and the solutions were incubated at rt for 7 days. The stabilities were measured and analyzed by radio-HPLC to determine the stability as a function of time. Corresponding stabilities of (*R*)- and (*S*)-[<sup>68</sup>Ga]Ga-13 were also evaluated in PBS and similarly analyzed by HPLC at 2 h at room temperature (rt) after the preparation.

**Cell Culture and Tumor Mouse Models.** PC3-PIP<sup>38</sup> (PSMA-positive, (generously provided by Dr. Sean Carlin, University of Pennsylvania)) and PC3 (PSMA-negative, purchased from ATCC, American Type Culture Collection) cell lines<sup>39</sup> were used for cell uptake studies and inoculation in CD-1 nu/nu mice. The cells were cultured in the RPMI 1640 medium supplemented with 10% fetal bovine serum and 1% antibiotics (penicillin/streptomycin) in a humidified incubator equilibrated with 5% CO<sub>2</sub> at 37 °C. After treatment with 0.25% trypsin with 0.02% EDTA and being resuspended in HBSS, each mouse was injected with 0.2 mL (5 × 10<sup>6</sup> cells) of the cell suspension in the left flank (PC3-PIP) or right flank (PC3).

Tumor-bearing mice were used for studies when tumor reached a diameter of approximately 5–10 mm.

**In Vitro Competition Binding Assays for PSMA Binding Affinity.** Assays were carried out by incubating PSMA-positive PC3-PIP cells with 0.2 nM, 3.7 MBq [<sup>125</sup>I]MIP-1095<sup>40</sup> (structure shown in Figure S10) in the presence of 10 different concentrations (10<sup>-5</sup>–10<sup>-10</sup> M) of competing “cold” ligands. Nonspecific binding (NSB) was defined with 2 μM PSMA-617. After incubation at 37 °C for 1 h, the bound and free fractions were separated by vacuum filtration through a GF/B filter paper using a Brandel M-24R cell harvester. The filters were washed twice with cold Tris–HCl buffer (50 mM, pH 7.4), and the radioactivity was counted in a gamma counter (Wizard2, PerkinElmer). The IC<sub>50</sub> values were calculated by GraphPad Prism.

**Cell Binding and Internalization.** PC3-PIP cells were cultured in 12-well plates 24 h before cell uptake studies (5 × 10<sup>5</sup> cells/well). After washing, the cells were incubated with 37 kBq of [<sup>68</sup>Ga]Ga-PSMA-093, (*R*)- and (*S*)-[<sup>68</sup>Ga]Ga-13, (*R*)- and (*S*)-[<sup>177</sup>Lu]Lu-13, and [<sup>177</sup>Lu]Lu-PSMA-617 for 5, 15, 30, 60, 90, and 120 min at 37 °C. At the indicated time, the medium was removed and the cells were washed twice with 1 mL of cold PBS. Cells were subsequently incubated twice with 1 mL of glycine–HCl in PBS (50 mM, pH 2.8) for 5 min to remove the surface-bound fraction. The cells were lysed using 0.1 mL of 1 N NaOH. The lysed cells were removed by filters and measured in a gamma counter. The cell uptake was calculated as percent of the initial dose bound to 10<sup>6</sup> cells [%ID/10<sup>6</sup> cells]. Experiments were performed in triplicate.

**Biodistribution Studies.** [<sup>68</sup>Ga]Ga-PSMA-093, [<sup>68</sup>Ga]Ga-PSMA-617, and (*R*)- and (*S*)-[<sup>68</sup>Ga]Ga-13 were injected (629 kBq, 0.16 nmol) via tail vein of PC-3 and PC3-PIP tumor-bearing nude mice. Organs of interest were dissected and weighed after the animals were sacrificed at 1 h. The radioactivity was measured with a gamma counter, and the % ID/g was calculated by comparison with samples of standard dilution of the initial dose. All measurements were corrected for decay.

## RESULTS AND DISCUSSION

**Syntheses of DOTAGA(<sup>t</sup>Bu)<sub>4</sub> ((*R*)-, (*S*)-, and (*R,S*)-9).** Syntheses of DOTAGA(<sup>t</sup>Bu)<sub>4</sub> ((*R*)-, (*S*)-, and (*R,S*)-9) were successfully achieved in two steps: synthesis of the mixture and chiral stereoselective side arms, 2 and (*S*)- and (*R*)-6, and synthesis of DOTAGA(<sup>t</sup>Bu)<sub>4</sub> (Schemes 1 and 2). Compound 2, containing a racemic side arm, was prepared from (*S*)-glutamic acid 5-methyl ester using a synthesis method reported previously.<sup>41</sup> The chirality at the C2 position of 1 was partially racemized during the displacement of bromide. Subsequently, the acid group was protected with TBTA (*tert*-butyl trichloroacetimide) to give (racemic)-2 in 80% yield. Compounds (*S*)- and (*R*)-6, containing a C2 chiral –OMs group, were prepared from the corresponding (*S*)- and (*R*)-glutamic acids, respectively.<sup>36,37,42</sup> Stereoselective preparation of (*S*)- and (*R*)-3 was achieved by addition of NaNO<sub>2</sub> solution to the excess HCl reaction solution containing either (*S*)- or (*R*)-glutamic acid at low temperature (between 0 and 5 °C). Under this condition, the C2 optical center retained the chirality. The corresponding <sup>t</sup>Bu-protected esters, (*S*)- and (*R*)-4, were synthesized in 87% yield using the optimized procedure described above. The reaction yields were better than those reported previously using 4-dimethylaminopyridine (DMAP) and *N,N'*-dicyclohexylcarbodiimide (DCC) as the catalyst.<sup>36</sup>

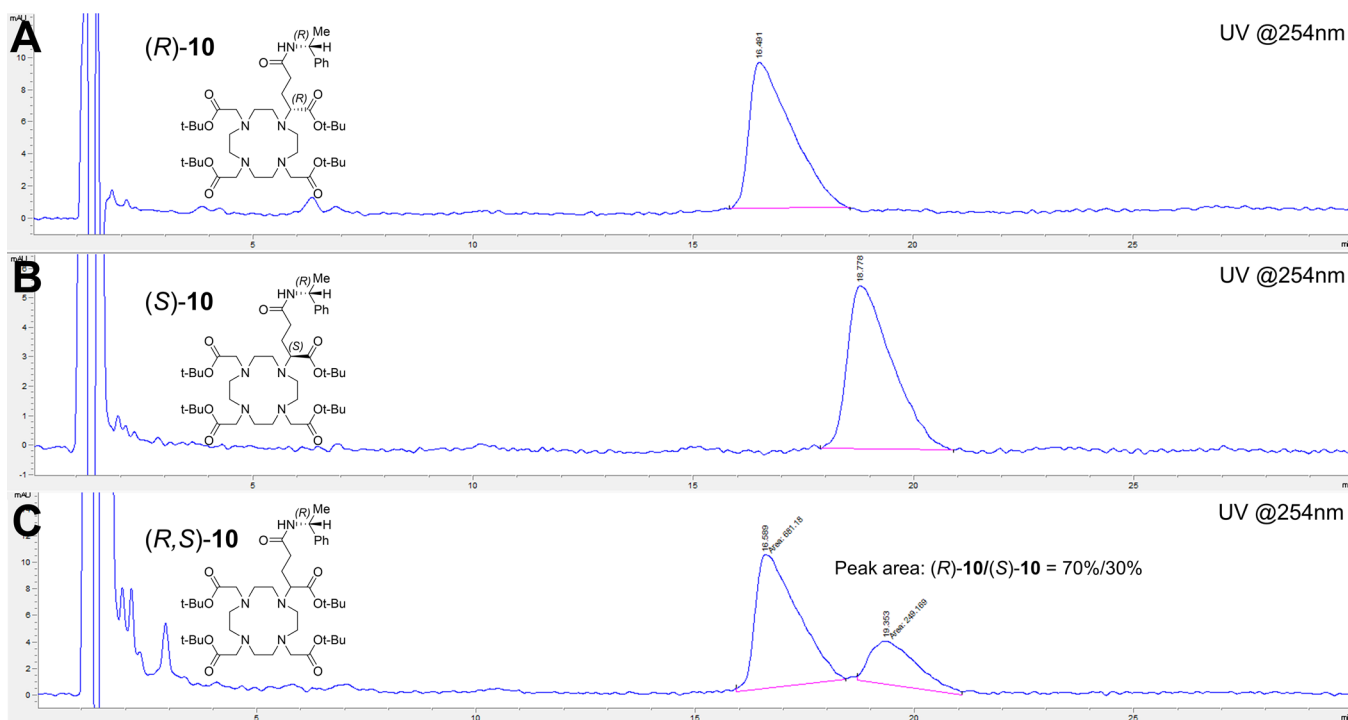


**Figure 3.** HPLC profiles of (R)-(+)- $\alpha$ -methylbenzylamide derivatives, (R)-, (S)-, and (R,S)-10, under the following conditions: PRP-1 10  $\mu$ m, 250  $\times$  4.6 mm column, ACN/0.5% TFA in water = 4/6, 2 mL/min, and 10  $^{\circ}$ C. (A, B) Two stereoisomers (R)-10 (A) and (S)-10 (B) separated under these conditions with retention times of 16 and 19 min, respectively. (C) Prepared mixture of (R,S)-10 showed a 7 to 3 ratio of R to S. The corresponding NMR spectroscopic data also support the conclusion. (NMR data of (R)-(+)- $\alpha$ -methylbenzylamide derivatives, (R)-, (S)-, and (R,S)-10, are included in the Supporting Information; Figures S1–S3.)

(S)- and (R)-4 were subjected to the lactone ring opening by sodium methoxide (NaOMe) in MeOH at 0  $^{\circ}$ C for 30 min to give (S)- and (R)-5 in 77% yield. This one-step lactone ring opening with NaOMe was faster and easier to handle than the KOH hydrolysis and benzyl protection as reported earlier.<sup>36</sup> Finally, the secondary alcohols, (S)- and (R)-5, were stereoselectively converted to the corresponding mesylates to provide (S)- and (R)-6, respectively. Mesylate was chosen as the leaving group because the controlled alkylation of cyclen by the S<sub>N</sub>2 reaction afforded a complete inversion of stereochemistry at the C2 optical center of the glutamic acid side arm. The desired products, DOTAGA(<sup>t</sup>Bu)<sub>4</sub> ((R)- and (S)-9), were readily prepared in three steps in 30% yield.

The optical purity of DOTAGA(<sup>t</sup>Bu)<sub>4</sub> ((R)-, (S)-, and (R,S)-9), prepared above was not easily determined. The synthesis employed optically defined precursors, 2, (S)-6, and (R)-6, through which presumably optically specific (R)-, (S)-, and (R,S)-9 were prepared (Schemes 1 and 2). However, the specific optical purities of (R)-, (S)-, and (R,S)-9 cannot be easily measured by HPLC as they are enantiomers and lack a chromophore. To add a suitable chromophore and enhance optical characteristics, small samples of (R)-, (S)-, and (R,S)-9 were converted to diastereomeric (R)-(+)- $\alpha$ -methylbenzylamide derivatives, (R)-, (S)-, and (R,S)-10, respectively. The HPLC profiles showed that the chiral purity ((R)-10 and (S)-10) was >99%, and the racemic DOTAGA(<sup>t</sup>Bu)<sub>4</sub>, (R,S)-10 was a 70%/30% (R/S) mixture of diastereomers (Figure 3). Additionally, the <sup>1</sup>H NMR spectrum of (R,S)-10 also indicated that it is consisted of a 70%/30% racemic mixture according to the ratio of the NH proton on (R,S)-10 (Figures S1–S3). The same starting materials were also employed for synthesis of optically pure (R)- and (S)-13. It is expected that the optically pure (R)-

and (S)-13 will be prepared as described above, and they will show similar optical purity that described above for (R)-10 and (S)-10, respectively (Scheme 3).

**Synthesis of [<sup>nat</sup>Ga]Ga- and [<sup>nat</sup>Lu]Lu-DOTAGA-PSMA-093, (R)-[<sup>nat</sup>Ga]Ga-13, (R)-[<sup>nat</sup>Lu]Lu-13, (S)-[<sup>nat</sup>Ga]Ga-13, and (S)-[<sup>nat</sup>Lu]Lu-13.** Synthetic schemes of unlabeled reference ligands, (R)-[<sup>nat</sup>Ga]Ga-13, (R)-[<sup>nat</sup>Lu]Lu-13, (S)-[<sup>nat</sup>Ga]Ga-13, and (S)-[<sup>nat</sup>Lu]Lu-13 complexes, are summarized in Scheme 3. The key intermediate compound 11, containing the linker and the PSMA binding group, –Glu-NH-CO-NH-Lys, was prepared as previously reported.<sup>29</sup> Compounds (R)- and (S)-12 were prepared by a coupling reaction of DOTAGA(<sup>t</sup>Bu)<sub>4</sub>, (R)- and (S)-9, in 78 and 51%, respectively. After removing *tert*-butyl protection groups by TFA to give compounds (R)- and (S)-13 in 54 and 41% yields, respectively, (LC–MS profiles are shown in Figures S4 and S5, respectively.) the desired precursors (R)- and (S)-13 were used for radiolabeling of [<sup>68</sup>Ga]Ga-13 and [<sup>177</sup>Lu]Lu-13 and synthesis of “cold” compounds, [<sup>nat</sup>Ga]Ga-13 and [<sup>nat</sup>Lu]Lu-13 (LC–MS profiles are shown in Figures S6–S9). Unfortunately, attempts in making the corresponding crystals for structural determination of the chelates, (R)- and (S)-13, and the corresponding metal (<sup>nat</sup>Ga and <sup>nat</sup>Lu) complexes were not successful; this part of the work remains to be accomplished in the future.

**Radiosynthesis of [<sup>68</sup>Ga]Ga- and [<sup>177</sup>Lu]Lu-DOTAGA-PSMA-093, (R)-[<sup>68</sup>Ga]Ga-13, (R)-[<sup>177</sup>Lu]Lu-13, (S)-[<sup>68</sup>Ga]Ga-13, (S)-[<sup>177</sup>Lu]Lu-13, and [<sup>68</sup>Ga]Ga/[<sup>177</sup>Lu]Lu-PSMA-617.** Gallium-68 was obtained from a <sup>68</sup>Ge/<sup>68</sup>Ga generator (ITG, Germany), and lutetium-177 was obtained from the National Isotope Development Center, Oak Ridge National Laboratory (Oak Ridge, TN). Initially, it was determined that complex formation of (R)- and (S)-[<sup>68</sup>Ga]Ga-

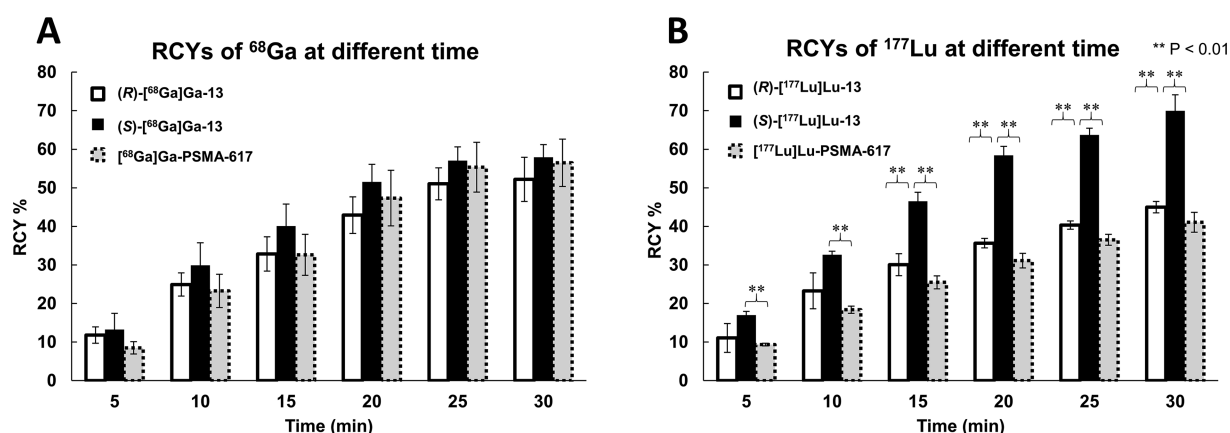


**Figure 4.** (A, B) Kinetics of complex formation was measured at 50 °C for (R)- and (S)-[<sup>68</sup>Ga]Ga-13 and [<sup>68</sup>Ga]Ga-PSMA-617 (A) and (R)- and (S)-[<sup>177</sup>Lu]Lu-13 and [<sup>177</sup>Lu]Lu-PSMA-617 (B). Radiochemical yield (RCY) was determined by the TLC method ( $n = 3$ ) (\*\*statistically  $p < 0.01$ ). The formation of (S)-[<sup>177</sup>Lu]Lu-13 displayed a much faster rate than those of (R)-[<sup>177</sup>Lu]Lu-13 and [<sup>177</sup>Lu]Lu-PSMA-617. This suggests that the stereochemistry of the extra glutamic acid arm on <sup>177</sup>Lu-DOTAGA in combination with the stereochemistry of the linker and PSMA part played an important role in complex formation. Results presented in this section clearly demonstrate that the speed of <sup>177</sup>Lu-DOTAGA-PSMA-093 complex formation is dependent on the stereochemistry of the extra glutamic acid arm.

13, (R)- and (S)-[<sup>177</sup>Lu]Lu-13, and [<sup>68</sup>Ga]Ga/[<sup>177</sup>Lu]Lu-PSMA-617 were readily accomplished in a few minutes at reaction temperature above 80 °C. To study the effect of stereoselective isomers on the kinetics of complex formation, labeling was performed at 50 °C, a temperature in which the kinetics of complex formation was sufficiently slow and measurable at different time points. As shown in Figure 4, the labeling yields of (R)- and (S)-[<sup>68</sup>Ga]Ga-13, (R)- and (S)-[<sup>177</sup>Lu]Lu-13, and [<sup>68</sup>Ga]Ga/[<sup>177</sup>Lu]Lu-PSMA-617 increased over 30 min. The formation of (S)-[<sup>68</sup>Ga]Ga-13, the (S)-DOTAGA chelator, displayed a small but noticeable faster kinetics in comparison with (R)-[<sup>68</sup>Ga]Ga-13 and [<sup>68</sup>Ga]Ga-PSMA-617, the (R)-DOTAGA and DOTA chelators, respectively. Meanwhile, the formation of (S)-[<sup>177</sup>Lu]Lu-13 showed significantly faster kinetics in comparison with (R)-[<sup>177</sup>Lu]Lu-13 and [<sup>177</sup>Lu]Lu-PSMA-617, and the (R)-[<sup>177</sup>Lu]Lu-13 also showed a noticeable faster complex rate compared with [<sup>177</sup>Lu]Lu-PSMA-617. It appeared that (S)-DOTAGA was the preferred isomer showing a clearly faster rate of <sup>177</sup>Lu complex formation and a negligible faster rate of <sup>68</sup>Ga complex formation in comparison with (R)-DOTAGA and DOTA. Unlike the six coordination of Ga(III)-DOTAGA, the coordination of Lu(III) with DOTAGA prefer nine-coordinate covalent bonds, which would be affected by the stereochemistry of an extra glutamic acid arm.

For routine preparations, (R)- and (S)-[<sup>68</sup>Ga]Ga-13 were successfully prepared at 80 °C by mixing [<sup>68</sup>Ga]GaCl<sub>3</sub> in 0.05 M HCl with 20 μg of (R)- and (S)-13 in a NaOAc buffer (pH = 5) for 10 min. (R)- and (S)-[<sup>177</sup>Lu]Lu-13 and [<sup>177</sup>Lu]Lu-PSMA-617 were successfully prepared at 90 °C by mixing [<sup>177</sup>Lu]LuCl<sub>3</sub> in 0.05 M HCl with 10 μg of (R)- and (S)-13 in a NaOAc buffer (pH = 5) for 20 min. Radiochemical purities were consistently >95%, which were confirmed by radio-HPLC analysis.

Another example of adding (R)- or (S)-glutamic acid arms on DOTA in developing MRI contrast agents has been reported.<sup>43,44</sup> The importance of the glutamic acid arm and its optical isomers ((R)- vs (S)-glutamic isomers) on the stability and in vivo kinetics of Gd-DOTAGA vs DOTA was not trivial, and its significance has been identified and evaluated.<sup>43–45</sup> It was discovered that there were major differences between Gd-DOTA and Gd-DOTAGA. The adjacent glutamic acid arm of

Gd-DOTAGA was amenable to conjugation to a variety of chemical moieties. More importantly, the additional arm on DOTAGA introduced by adding one or more glutamic acid groups enhanced rotational immobilization and provided a large enhancement of magnetic relaxivity and stability.<sup>43–45</sup> Similarly, lanthanide complexes of DOTA containing four glutamic arms, resulting in adding four optical centers, have been reported. The results of complex formation analysis and quantum mechanical calculations for the Ln-DOTA(GA)<sub>4</sub> complexes suggested that there was a rapid formation of metastable species, consisting of multiple isomeric forms, leading to a slow formation and reorganization of the macrocycle. Specifically, greater stability of these final Gd(III) complexes resulted from formation of transitory bonds between the metal ion and pendant glutamic arms, which contained four carboxylate groups. One major improvement of adding glutamic arms on DOTA(GA)<sub>x</sub> (where  $x = 1$  to 4) for chelating Gd(III) was that the stability constants of the final complexes had higher values than those for DOTA without the added glutamic acid arms.<sup>46</sup> It is reasonable to conclude that there were at least two major advantages of DOTAGA compared to DOTA: (1) faster kinetics of forming Gd-DOTAGA complex(es) and (2) enhanced stability provided by the additional glutamic arms.<sup>47</sup> There were suggestions of differences in the rate of formation and transition between different stereoisomers; however, the extent of such effects was not fully evaluated.<sup>46,47</sup> We expect that these findings would likely be consistent with the complex formation of Ga/Lu-DOTAGA and would perhaps also be applicable to many other 3+ charged metals.<sup>8</sup>

**In Vitro Stability in PBS and Plasma.** The stabilities of (R)- and (S)-[<sup>177</sup>Lu]Lu-13, synthesized by routine preparations, were investigated by incubation in PBS and in plasma at 37 °C. After incubation for 7 days, the radiochemical purities remained unchanged, maintaining a stable RCP of approximately >90%. (Radio-HPLC profiles are shown in the Supporting Information, Figures S10 and S11, respectively). Release of <sup>177</sup>Lu from complexes was not observed under respective experimental conditions in the examined time. As expected, (R)- and (S)-[<sup>177</sup>Lu]Lu-13 were stable in PBS without any measurable decomposition. HPLC profiles of (R)- and (S)-[<sup>68</sup>Ga]Ga-13

suggested that they were stable in PBS at room temperature 2 h after preparation.

**In Vitro Assay for PSMA Binding Affinity.** The PSMA binding affinities of  $^{nat}\text{Ga}$  and  $^{nat}\text{Lu}$  analogues were determined in competitive binding assays using PC3-PIP cell homogenates and [ $^{125}\text{I}$ ]MIP-1095 (structure shown in Figure S12), a known PSMA radiotracer as the “hot” ligand for competition.<sup>40</sup> The relatively long half-life of  $^{125}\text{I}$  ( $t_{1/2}$ , 60 days) makes it simple by preparing one batch of [ $^{125}\text{I}$ ]MIP-1095 for multiple experiments. The  $\text{IC}_{50}$  values (mean  $\pm$  SD) are summarized in Table 1.

**Table 1. Binding Affinities to PSMA ( $\text{IC}_{50}$  Values, Mean  $\pm$  SD,  $n = 4$ )<sup>a</sup>**

ligands	$\text{IC}_{50}$ (nM)
MIP-1095	5.4 $\pm$ 1.0
PSMA-093	13.0 $\pm$ 0.7
[ $^{nat}\text{Ga}$ ]Ga-PSMA-093	34.0 $\pm$ 4.5
( <i>R</i> )-13	24.2 $\pm$ 2.8
( <i>S</i> )-13	45.7 $\pm$ 9.4
( <i>R</i> )-[ $^{nat}\text{Ga}$ ]Ga-13	58.4 $\pm$ 38.9
( <i>S</i> )-[ $^{nat}\text{Ga}$ ]Ga-13	111.3 $\pm$ 26.3
( <i>R</i> )-[ $^{nat}\text{Lu}$ ]Lu-13	46.3 $\pm$ 13.5
( <i>S</i> )-[ $^{nat}\text{Lu}$ ]Lu-13	68.1 $\pm$ 13.9

<sup>a</sup>Binding assays were carried out using PC3-PIP cell homogenates and [ $^{125}\text{I}$ ]MIP-1095<sup>40</sup> as the “hot” ligand for competition.

(The detailed data are shown in Table S1.) All of (*S*)- and (*R*)-13 and corresponding  $^{nat}\text{Ga}$  and  $^{nat}\text{Lu}$  equivalents displayed high binding affinity ( $\text{IC}_{50} = 24\text{--}111$  nM), values comparable or slightly higher than that of the parent agent, [ $^{nat}\text{Ga}$ ]Ga-PSMA-093 ( $\text{IC}_{50} = 34.0 \pm 4.5$  nM). (*S*)-13, showed a slightly lower affinity than (*R*)-13 ( $\text{IC}_{50}$  values of  $45.7 \pm 9.4$  vs  $24.2 \pm 2.8$  nM, respectively). In addition, the inhibition potency for the isomeric pair, (*R*)- and (*S*)-[ $^{nat}\text{Ga}$ ]Ga-13 and (*R*)- and (*S*)-[ $^{nat}\text{Lu}$ ]Lu-13 demonstrated different  $\text{IC}_{50}$  values ( $58.4 \pm 38.9$  vs  $111.3 \pm 26.3$  nM and  $46.3 \pm 13.5$  vs  $68.1 \pm 13.9$  nM, respectively). It is apparent that the (*R*)-isomers displayed slightly higher binding affinity in comparison with the (*S*)-isomers, and all values were in the same order of magnitude.

Therefore, the (*S*)- and (*R*)-DOTAGA chelating groups showed no significant influence in the PSMA binding affinity. This is likely due to the fact that the binding pocket is far away from the urea-binding moiety, which is the moiety responsible for PSMA binding.

**Cell Binding and Internalization Study.** In vitro cell binding and specific internalization (PC3-PIP cells over-expressing PSMA) were determined using [ $^{68}\text{Ga}$ ]Ga-PSMA-093 and [ $^{177}\text{Lu}$ ]Lu-PSMA-617 as known controls, respectively. The cell binding and internalization of  $^{68}\text{Ga}$ -ligands and  $^{177}\text{Lu}$ -ligands increased over incubation time. (Complete results are presented in Figure S4.) The total cell uptake values of  $^{68}\text{Ga}$ -ligands, (*R*)- and (*S*)-[ $^{68}\text{Ga}$ ]Ga-13 and [ $^{68}\text{Ga}$ ]Ga-PSMA-093, were comparable (18.4, 14.5, and 17.4% ID/ $10^6$  cells at 1 h; 25.3, 22.5, and 29.8% ID/ $10^6$  cells at 2 h, respectively), while [ $^{68}\text{Ga}$ ]Ga-PSMA-093 showed a significantly higher internalization in comparison with (*R*)- and (*S*)-[ $^{68}\text{Ga}$ ]Ga-13 (12.0, 5.8, and 5.5% ID/ $10^6$  cells at 1 h; 21.9, 11.2, and 9.5% ID/ $10^6$  cells at 2 h, respectively). This is likely due to the fact that the advantage of HBED-CC aromatic stacking improved the internalization (Figure 5A). (*R*)- and (*S*)-[ $^{177}\text{Lu}$ ]Lu-13 and [ $^{177}\text{Lu}$ ]Lu-PSMA-617 displayed comparable total cell uptake (20.2, 20.6, and 20.0% ID/ $10^6$  cells at 1 h; 24.2, 23.3, and 24.7% ID/ $10^6$  cells at 2 h, respectively) and internalization (7.4, 7.2, and 7.3% ID/ $10^6$  cells at 1 h; 10.9, 10.8, and 11.3% ID/ $10^6$  cells at 2 h, respectively) (Figure 5B). It is apparent that (*R*)- and (*S*)-DOTAGA-based [ $^{68}\text{Ga}$ ]/[ $^{177}\text{Lu}$ ]-13 displayed negligible isomeric effect on the cell uptake studies. Evidently, [ $^{68}\text{Ga}$ ]Ga-PSMA-093 was the only agent displaying a much higher internalization in the PSMA-expressing cells under the same condition.

#### In Vivo Biodistribution Study in Tumor-Bearing Mice.

A comparison of the biodistribution (1 h p.i.) of [ $^{68}\text{Ga}$ ]Ga-PSMA-093, [ $^{68}\text{Ga}$ ]Ga-PSMA-617, and (*R*)- and (*S*)-[ $^{68}\text{Ga}$ ]Ga-13 in male nude mice bearing PSMA-positive PC3-PIP and PSMA-negative PC-3 tumors is summarized in Table 2.

The biodistribution data between [ $^{68}\text{Ga}$ ]Ga-PSMA-093, [ $^{68}\text{Ga}$ ]Ga-PSMA-617, and (*R*)- and (*S*)-[ $^{68}\text{Ga}$ ]Ga-13 displayed comparable values. There was higher uptake of (*R*)- and (*S*)-[ $^{68}\text{Ga}$ ]Ga-13 in the PSMA-expressing PC3-PIP xenograft tumors in mice ( $12.1 \pm 1.91$  and  $13.3 \pm 0.39\%$  ID/g,

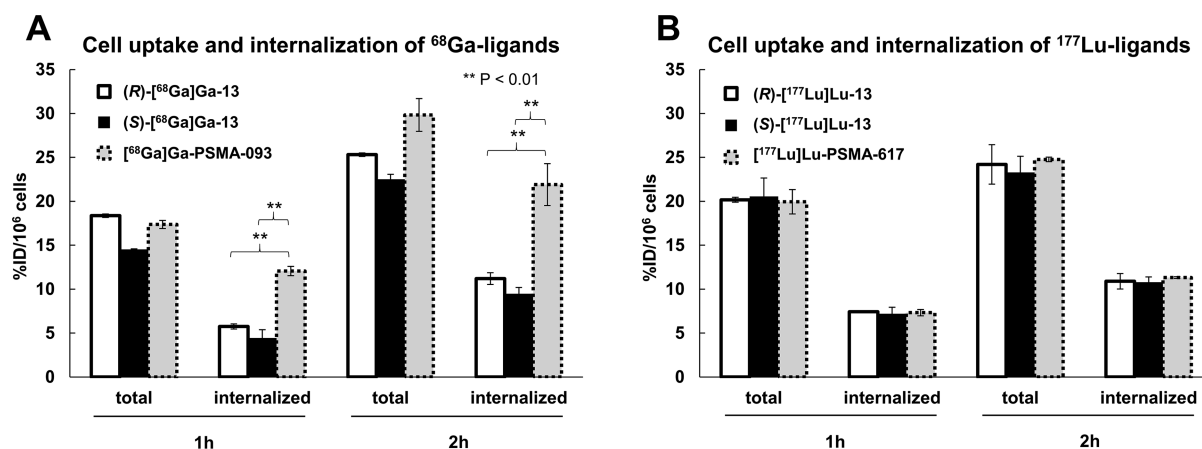


**Figure 5.** Cell uptake and internalization of  $^{68}\text{Ga}$ - and  $^{177}\text{Lu}$ -labeled compounds were evaluated in PC3-PIP cells for 1 and 2 h of incubation ( $n = 3$ ). Values are expressed as percent of the initial dose bound to  $10^6$  cells [% ID/ $10^6$  cells] (\*\*statistically  $p < 0.01$ ). (A) (*R*)-[ $^{68}\text{Ga}$ ]Ga-13 (white), (*S*)-[ $^{68}\text{Ga}$ ]Ga-13 (black), and [ $^{68}\text{Ga}$ ]Ga-PSMA-093 (gray) were evaluated in PC3-PIP cells for 1 and 2 h of incubation. (*R*)-[ $^{68}\text{Ga}$ ]Ga-13 (white) and (*S*)-[ $^{68}\text{Ga}$ ]Ga-13 (black) showed very similar uptake values. Internalization values of [ $^{68}\text{Ga}$ ]Ga-PSMA-093 at 1 and 2 h were much higher than those of (*R*)-[ $^{68}\text{Ga}$ ]Ga-13 (white) and (*S*)-[ $^{68}\text{Ga}$ ]Ga-13 (black). (B) (*R*)-[ $^{177}\text{Lu}$ ]Lu-13 (white), (*S*)-[ $^{177}\text{Lu}$ ]Lu-13 (black), and [ $^{177}\text{Lu}$ ]Lu-PSMA-617 (gray) showed very similar cell uptake values at 1 and 2 h. Results of more detailed kinetics are shown in Figure S13 (Supporting Information).

**Table 2. Biodistribution at 1 h Post-Injection in Tumor-Bearing Mice of [<sup>68</sup>Ga]Ga-PSMA-093, [<sup>68</sup>Ga]Ga-PSMA-617, and (R)- and (S)-[<sup>68</sup>Ga]Ga-13 (% ID/g, Avg ± SD, n = 3)**

part	[ <sup>68</sup> Ga]Ga-PSMA-093	[ <sup>68</sup> Ga]Ga-PSMA-617	(R)-[ <sup>68</sup> Ga]Ga-13	(S)-[ <sup>68</sup> Ga]Ga-13
blood	0.64 ± 0.10	0.44 ± 0.11	0.86 ± 0.09	1.54 ± 0.07
heart	0.63 ± 0.09	0.15 ± 0.04	0.45 ± 0.16	0.57 ± 0.12
muscle	0.68 ± 0.39	0.11 ± 0.03	0.29 ± 0.04	0.35 ± 0.04
lung	2.37 ± 0.70	0.55 ± 0.15	1.18 ± 0.13	1.57 ± 0.04
kidney	165.1 ± 50.1	25.6 ± 31.5	144.6 ± 16.2	131.4 ± 1.43
spleen	20.0 ± 13.2	0.86 ± 0.32	2.52 ± 0.70	2.80 ± 0.23
pancreas	1.32 ± 0.58	0.18 ± 0.12	0.76 ± 0.18	1.13 ± 0.62
liver	0.94 ± 0.34	1.94 ± 0.57	0.34 ± 0.03	0.56 ± 0.04
stomach	0.60 ± 0.54	0.06 ± 0.01	0.33 ± 0.15	0.62 ± 0.14
skin	1.56 ± 0.35	0.36 ± 0.19	0.85 ± 0.29	1.23 ± 0.20
bone	0.31 ± 0.06	0.09 ± 0.03	0.50 ± 0.23	0.43 ± 0.02
PC3-PIP tumor <sup>a</sup>	19.2 ± 5.66	10.1 ± 1.84	12.1 ± 1.91	13.3 ± 0.39
PC-3 tumor <sup>a</sup>	1.77 ± 0.63	0.50 ± 0.30	0.96 ± 0.05	1.41 ± 0.03

<sup>a</sup>PC-3 (PSMA<sup>-</sup>)/PC3-PIP (PSMA<sup>+</sup>) cells were implanted in nude mice.<sup>39</sup>

respectively) compared to [<sup>68</sup>Ga]Ga-PSMA-617 (uptake in PC3-PIP tumor was 10.1 ± 1.84 %ID/g), while there was very low uptake in PC-3 tumor (PSMA negative). The new PSMA agents, (R)- and (S)-[<sup>68</sup>Ga]Ga-13, clearly displayed a 30% lower tumor uptake than [<sup>68</sup>Ga]Ga-PSMA-093 and 20% higher than [<sup>68</sup>Ga]Ga-PSMA-617. All PSMA-093 ligands, [<sup>68</sup>Ga]Ga-PSMA-093 and (R)- and (S)-[<sup>68</sup>Ga]Ga-13, showed higher kidney uptake compared with [<sup>68</sup>Ga]Ga-PSMA-617 (165.1 ± 50.1, 144.6 ± 16.2, 131.4 ± 1.43, and 25.6 ± 31.5% ID/g, respectively). However, <sup>177</sup>Lu-ligands showed much lower kidney uptake compared with <sup>68</sup>Ga-ligands as previous reported.<sup>48</sup> It is likely due to the fact that the PSMA-targeting properties of [<sup>177</sup>Lu]Lu-13 are comparable to those of [<sup>177</sup>Lu]Lu-PSMA-617, a theragnostic ligand currently in clinical evaluation. The K<sub>i</sub> of [<sup>177</sup>Lu]Lu-PSMA-617 was reported as being 2.34 ± 2.94 nM determined with LNCaP cells, while our studies of [<sup>177</sup>Lu]Lu-13 were measured with PSMA-expressing PC3-PIP cells.<sup>49</sup> Apparently, the in vivo biodistribution was not affected by the optical isomer formation for <sup>68</sup>Ga/<sup>177</sup>Lu-DOTAGA complexes. However, in vivo stability of these isomers in humans needs to be evaluated further in the future.

More recently, a radiohybrid PSMA-targeting agent, rhPSMA-7.3, was reported (see Figure 2).<sup>30–33</sup> A phase 3 “SPOTLIGHT” trial, which examines the investigational PSMA-targeting PET imaging agent, rhPSMA-7.3 F18, in men with suspected prostate cancer recurrence, was recently announced by Blue Earth Diagnostic Inc. It is noted that the glutamic acid arm of the DOTAGA chelating group of rhPSMA-7.3 is reported to be the (S)-isomer.

## CONCLUSIONS

In summary, new PSMA-targeting agents were prepared by combining stereoselective (R)- and (S)-DOTAGA chelators and the PSMA-093 (without HBED) moiety. Resulting optically pure isomers, (R)- and (S)-[<sup>68</sup>Ga/<sup>177</sup>Lu]-13, showed comparable PSMA-targeting properties. However, the formation of (S)-[<sup>177</sup>Lu]Lu-13 showed significantly faster labeling kinetics than that of (R)-[<sup>177</sup>Lu]Lu-13, demonstrating a clear stereo effect of (R)- and (S)-DOTAGA-PSMA-093 on <sup>177</sup>Lu chelation. The (S)-DOTAGA-PSMA ligand, (S)-13, may serve as a useful candidate ligand for developing diagnostic and therapeutic agents targeting PSMA binding in tumors. Although there are no differences in PSMA targeting between (R)- and (S)-DOTAGA isomers, their differences in forming metal complexes are

noteworthy and should not be ignored in preparation of <sup>177</sup>Lu-DOTAGA derivatives for future applications.

## ASSOCIATED CONTENT

### Supporting Information

The Supporting Information is available free of charge at <https://pubs.acs.org/doi/10.1021/acs.molpharmaceut.0c00777>.

Synthesis of compounds 2 and (R)-6, <sup>1</sup>H NMR of compound (R,S)-10, <sup>1</sup>H NMR of compound (R)-10, <sup>1</sup>H NMR of compound (S)-10, LC–MS of compound (R)-13, LC–MS of compound (S)-13, LC–MS of compound (R)-[<sup>nat</sup>Ga]Ga-13, LC–MS of compound (S)-[<sup>nat</sup>Ga]Ga-13, LC–MS of compound (R)-[<sup>nat</sup>Lu]Lu-13, LC–MS of compound (S)-[<sup>nat</sup>Lu]Lu-13, radio-HPLC profile of (R)-[<sup>177</sup>Lu]Lu-13 and stability in PBS and plasma, radio-HPLC profile of (S)-[<sup>177</sup>Lu]Lu-13 and stability in PBS and plasma, structure of [<sup>125</sup>I]MIP-1095 and IC<sub>50</sub> values, and cell uptake and internalization of <sup>68</sup>Ga- and <sup>177</sup>Lu-labeled compounds (PDF)

## AUTHOR INFORMATION

### Corresponding Author

Hank F. Kung – Department of Radiology, University of Pennsylvania, Philadelphia, Pennsylvania 19104, United States; Five Eleven Pharma Inc., Philadelphia, Pennsylvania 19104, United States; Email: [kunghf@gmail.com](mailto:kunghf@gmail.com)

### Authors

Ruiyue Zhao – College of Chemistry, Beijing Normal University, Beijing 100875, PR China

Karl Ploessl – Five Eleven Pharma Inc., Philadelphia, Pennsylvania 19104, United States; [orcid.org/0000-0001-7896-5900](https://orcid.org/0000-0001-7896-5900)

Zhihao Zha – Five Eleven Pharma Inc., Philadelphia, Pennsylvania 19104, United States

Seokrye Choi – Five Eleven Pharma Inc., Philadelphia, Pennsylvania 19104, United States

David Alexoff – Five Eleven Pharma Inc., Philadelphia, Pennsylvania 19104, United States

Lin Zhu – College of Chemistry, Beijing Normal University, Beijing 100875, PR China; [orcid.org/0000-0001-9530-8531](https://orcid.org/0000-0001-9530-8531)

Complete contact information is available at:

<https://pubs.acs.org/10.1021/acs.molpharmaceut.0c00777>

## Notes

The authors declare the following competing financial interest(s): This work was supported by Five Eleven Pharma Inc. I am the founder of this company.

## ACKNOWLEDGMENTS

Five Eleven Pharma, Inc. was the sponsor of this study.

## ABBREVIATIONS

PSMA, prostate-specific membrane antigen; DTPA, diethylenetriaminepentaacetic acid; AAZTA, 6-[bis(hydroxycarbonylmethyl)amino]-1,4-bis(hydroxycarbonylmethyl)-6-methylperhydro-1,4-diazepine; TRAP, 1,4,7-triazacyclononane-1,4,7-triyltris(methylenephosphonic acid); DEDPA, 6,6'-[1,2-ethanediybis(iminomethylene)]bis[2-pyridinecarboxylic acid]; NOTA, 1,4,7-triazacyclononane-1,4,7-triacetic acid; DOTA, 1,4,7,10-tetraazacyclododecane-1,4,7,10-tetraacetic acid; DO3AM, 2-(4,7,10-tris(2-amino-2-oxoethyl)-1,4,7,10-tetraazacyclododecan-1-yl)acetic acid; NOTAGA, 1,4,7-triazacyclononane-1-glutaric acid-4,7-acetic acid; DOTAGA,  $\alpha$ -(2-carboxyethyl)-1,4,7,10-tetraazacyclododecane-1,4,7,10-tetraacetic acid; HBED-CC,  $N,N'$ -bis[2-hydroxy-5(carboxyethyl)-benzyl]ethylenediamine- $N,N'$ -diacetic acid

## REFERENCES

- (1) Velikyan, I.  $^{68}\text{Ga}$ -Based Radiopharmaceuticals: Production and Application Relationship. *Molecules* **2015**, *20*, 12913–12943.
- (2) Waterhouse, N. N.; Amor-Coarasa, A.; Nikolopoulou, A.; Babich, J. W. Otto: a 4.04 GBq (109 mCi)  $^{68}\text{Ge}/^{68}\text{Ga}$  generator, first of its kind - extended quality control and performance evaluation in the clinical production of [ $^{68}\text{Ga}$ ]Ga-PSMA-11. *EJNMMI Radiopharm. Chem.* **2020**, *5*, 5.
- (3) Prince, D.; Rossouw, D.; Rubow, S. Optimization of a Labeling and Kit Preparation Method for Ga-68 Labeled DOTATATE, Using Cation Exchange Resin Purified Ga-68 Eluates Obtained from a Tin Dioxide  $^{68}\text{Ge}/^{68}\text{Ga}$  Generator. *Mol. Imaging Biol.* **2018**, *20*, 1008–1014.
- (4) Hennrich, U.; Kopka, K. Lutathera<sup>®</sup>: The First FDA- and EMA-Approved Radiopharmaceutical for Peptide Receptor Radionuclide Therapy Lutetium lu 177 dotatate (Lutathera) for gastroenteropancreatic neuroendocrine tumors. *Pharmaceutics* **2019**, *12*, 114–e153.
- (5) Emmett, L.; Crumbaker, M.; Ho, B.; Willowson, K.; Eu, P.; Ratnayake, L.; Epstein, R.; Blanksby, A.; Horvath, L.; Guminski, A.; Mahon, K.; Gedye, C.; Yin, C.; Stricker, P.; Joshua, A. M. Results of a Prospective Phase 2 Pilot Trial of  $^{177}\text{Lu}$ -PSMA-617 Therapy for Metastatic Castration-Resistant Prostate Cancer Including Imaging Predictors of Treatment Response and Patterns of Progression. *Clin. Genitourin. Cancer* **2019**, *17*, 15–22.
- (6) Paganelli, G.; Sarnelli, A.; Severi, S.; Sansovini, M.; Belli, M. L.; Monti, M.; Foca, F.; Celli, M.; Nicolini, S.; Tardelli, E.; Marini, L.; Matteucci, F.; Giganti, M.; Di Iorio, V.; De Giorgi, U. Dosimetry and safety of  $^{177}\text{Lu}$  PSMA-617 along with polyglutamate parotid gland protector: preliminary results in metastatic castration-resistant prostate cancer patients. *Eur. J. Nucl. Med. Mol. Imaging* **2020**, DOI: 10.1007/s00259-020-04856-1.
- (7) Price, E. W.; Orvig, C. Matching chelators to radiometals for radiopharmaceuticals. *Chem. Soc. Rev.* **2014**, *43*, 260–290.
- (8) Kostelnik, T. I.; Orvig, C. Radioactive Main Group and Rare Earth Metals for Imaging and Therapy. *Chem. Rev.* **2018**, *119*, 902–956.
- (9) Kubíček, V.; Havlíčková, J.; Kotek, J.; Tircsó, G.; Hermann, P.; Tóth, E.; Lukeš, I. Gallium(III) complexes of DOTA and DOTAMonoamide: kinetic and thermodynamic studies. *Inorg. Chem.* **2010**, *49*, 10960–10969.

- (10) Wahsner, J.; Désogère, P.; Abston, E.; Graham-O'Regan, K. A.; Wang, J.; Ratile, N. J.; Schirmer, M. D.; Santos Ferreira, D. D.; Sui, J.; Fuchs, B. C.; Lanuti, M.; Caravan, P.  $^{68}\text{Ga}$ -NODAGA-Indole: An Allysine-Reactive Positron Emission Tomography Probe for Molecular Imaging of Pulmonary Fibrogenesis. *J. Am. Chem. Soc.* **2019**, *141*, 5593–5596.
- (11) Satpati, D.; Shinto, A.; Kamaleshwaran, K. K.; Sarma, H. D.; Dash, A. Preliminary PET/CT Imaging with Somatostatin Analogs [ $^{68}\text{Ga}$ ]DOTAGA-TATE and [ $^{68}\text{Ga}$ ]DOTAGA-TOC. *Mol. Imaging Biol.* **2017**, *19*, 878–884.
- (12) Choudhary, N.; de Guadalupe Jaraquemada-Peláez, M.; Zarschler, K.; Wang, X.; Radchenko, V.; Kubeil, M.; Stephan, H.; Orvig, C. Chelation in One Fell Swoop: Optimizing Ligands for Smaller Radiometal Ions. *Inorg. Chem.* **2020**, *59*, 5728–5741.
- (13) Herrmann, K.; Schwaiger, M.; Lewis, J. S.; Solomon, S. B.; McNeil, B. J.; Baumann, M.; Gambhir, S. S.; Hricak, H.; Weissleder, R. Radiotheranostics: a roadmap for future development. *Lancet Oncol.* **2020**, *21*, e146–e156.
- (14) Weineisen, M.; Schottelius, M.; Simecek, J.; Baum, R. P.; Yildiz, A.; Beykan, S.; Kulkarni, H. R.; Lassmann, M.; Klette, I.; Eiber, M.; Schwaiger, M.; Wester, H.-J.  $^{68}\text{Ga}$ - and  $^{177}\text{Lu}$ -Labeled PSMA I&T: Optimization of a PSMA-Targeted Theranostic Concept and First Proof-of-Concept Human Studies. *J. Nucl. Med.* **2015**, *56*, 1169–1176.
- (15) Weineisen, M.; Simecek, J.; Schottelius, M.; Schwaiger, M.; Wester, H. J. Synthesis and preclinical evaluation of DOTAGA-conjugated PSMA ligands for functional imaging and endoradiotherapy of prostate cancer. *EJNMMI Res.* **2014**, *4*, 63.
- (16) Cytawa, W.; Seitz, A. K.; Kircher, S.; Fukushima, K.; Tran-Gia, J.; Schirbel, A.; Bandurski, T.; Lass, P.; Krebs, M.; Polom, W.; Matuszewski, M.; Wester, H.-J.; Buck, A. K.; Kübler, H.; Lapa, C.  $^{68}\text{Ga}$ -PSMA I&T PET/CT for primary staging of prostate cancer. *Eur. J. Nucl. Med. Mol. Imaging* **2020**, *47*, 168–177.
- (17) Herrmann, K.; Bluemel, C.; Weineisen, M.; Schottelius, M.; Wester, H. J.; Czernin, J.; Eberlein, U.; Beykan, S.; Lapa, C.; Riedmiller, H.; Krebs, M.; Kropf, S.; Schirbel, A.; Buck, A. K.; Lassmann, M. Biodistribution and radiation dosimetry for a probe targeting prostate-specific membrane antigen for imaging and therapy. *J. Nucl. Med.* **2015**, *56*, 855–861.
- (18) Siegel, R. L.; Miller, K. D.; Jemal, A. Cancer statistics, 2019. *CA. Cancer J. Clin.* **2019**, *69*, 7–34.
- (19) Siegel, R. L.; Miller, K. D.; Jemal, A. Cancer statistics, 2020. *CA. Cancer J. Clin.* **2020**, *70*, 7–30.
- (20) Weber, M.; Kurek, C. E.; Barbato, F.; Eiber, M.; Maurer, T.; Nader, M.; Hadaschik, B.; Grünwald, V.; Herrmann, K.; Wetter, A.; Fendler, W. P. PSMA-ligand PET for early castration-resistant prostate cancer: a retrospective single-center study. *J. Nucl. Med.* **2020**, DOI: 10.2967/jnumed.120.245456.
- (21) Rowe, S. P.; Gorin, M. A.; Pomper, M. G. Imaging of Prostate-Specific Membrane Antigen with Small-Molecule PET Radiotracers: From the Bench to Advanced Clinical Applications. *Annu. Rev. Med.* **2019**, *70*, 461–477.
- (22) Derlin, T.; Schmuck, S.; Juhl, C.; Teichert, S.; Zörgiebel, J.; Wester, H.-J.; Schneefeld, S. M.; Walte, A. C. A.; Thackeray, J. T.; Ross, T. L.; Bengel, F. M. Imaging Characteristics and First Experience of [ $^{68}\text{Ga}$ ]THP-PSMA, a Novel Probe for Rapid Kit-Based Ga-68 Labeling and PET Imaging: Comparative Analysis with [ $^{68}\text{Ga}$ ]PSMA I&T. *Mol. Imaging Biol.* **2018**, *20*, 650–658.
- (23) Liu, C.; Liu, T.; Zhang, N.; Liu, Y.; Li, N.; Du, P.; Yang, Y.; Liu, M.; Gong, K.; Yang, X.; Zhu, H.; Yan, K.; Yang, Z.  $^{68}\text{Ga}$ -PSMA-617 PET/CT: a promising new technique for predicting risk stratification and metastatic risk of prostate cancer patients. *Eur. J. Nucl. Med. Mol. Imaging* **2018**, *45*, 1852–1861.
- (24) Perera, M.; Papa, N.; Roberts, M.; Williams, M.; Udovicich, C.; Vela, I.; Christidis, D.; Bolton, D.; Hofman, M. S.; Lawrentschuk, N.; Murphy, D. G. Gallium-68 Prostate-specific Membrane Antigen Positron Emission Tomography in Advanced Prostate Cancer-Updated Diagnostic Utility, Sensitivity, Specificity, and Distribution of Prostate-specific Membrane Antigen-avid Lesions: A Systematic Review and Meta-analysis. *Eur. Urol.* **2020**, *77*, 403–417.

- (25) Green, M. A.; Hutchins, G. D.; Bahler, C. D.; Tann, M.; Mathias, C. J.; Territo, W.; Sims, J.; Polson, H.; Alexoff, D.; Eckelman, W. C.; Kung, H. F.; Fletcher, J. W. [ $^{68}\text{Ga}$ ]Ga-P16-093 as a PSMA-Targeted PET Radiopharmaceutical for Detection of Cancer: Initial Evaluation and Comparison with [ $^{68}\text{Ga}$ ]Ga-PSMA-11 in Prostate Cancer Patients Presenting with Biochemical Recurrence. *Mol. Imaging Biol.* **2020**, *22*, 752–763.
- (26) Clarke, E. T.; Martell, A. E. 19. Stabilities of trivalent metal ion complexes of the tetraacetate derivatives of 12-, 13- and 14-membered tetraazamacrocycles. *Inorg. Chim. Acta* **1991**, *190*, 37–46.
- (27) Broan, C. J.; Cox, J. P. L.; Craig, A. S.; Katakya, R.; Parker, D.; Harrison, A.; Randall, A. M.; Ferguson, G. Structure and solution stability of indium and gallium complexes of 1,4,7-triazacyclononane-triacetate and yttrium complexes of 1,4,7,10-tetraazacyclododecane-triacetate and related ligands: kinetically stable complexes for use in imaging and radioimmunotherapy. X-ray molecular structure of the indium and gallium complexes of 1,4,7-triazacyclononane-1,4,7-triacetic acid. *J. Chem. Soc., Perkin Trans.* **1991**, *21*, 87–99.
- (28) Motekaitis, R. J.; Rogers, B. E.; Reichert, D. E.; Martell, A. E.; Welch, M. J. Stability and Structure of Activated Macrocycles. Ligands with Biological Applications. *Inorg. Chem.* **1996**, *35*, 3821–3827.
- (29) Zha, Z.; Ploessl, K.; Choi, S. R.; Wu, Z.; Zhu, L.; Kung, H. F. Synthesis and evaluation of a novel urea-based  $^{68}\text{Ga}$ -complex for imaging PSMA binding in tumor. *Nucl. Med. Biol.* **2018**, *59*, 36–47.
- (30) Kroenke, M.; Wurzer, A.; Schwamborn, K.; Ulbrich, L.; Jooss, L.; Maurer, T.; Horn, T.; Rauscher, L.; Haller, B.; Herz, M.; Wester, H. J.; Weber, W. A.; Eiber, M. Histologically Confirmed Diagnostic Efficacy of (18)F-rhPSMA-7 PET for N-Staging of Patients with Primary High-Risk Prostate Cancer. *J. Nucl. Med.* **2020**, *61*, 710–715.
- (31) Eiber, M.; Kroenke, M.; Wurzer, A.; Ulbrich, L.; Jooss, L.; Maurer, T.; Horn, T.; Schiller, K.; Langbein, T.; Buschner, G.; Wester, H. J.; Weber, W.  $^{18}\text{F}$ -rhPSMA-7 PET for the Detection of Biochemical Recurrence of Prostate Cancer After Radical Prostatectomy. *J. Nucl. Med.* **2020**, *61*, 696–701.
- (32) Wurzer, A.; Di Carlo, D.; Schmidt, A.; Beck, R.; Eiber, M.; Schwaiger, M.; Wester, H. J. Radiohybrid Ligands: A Novel Tracer Concept Exemplified by  $^{18}\text{F}$ - or  $^{68}\text{Ga}$ -Labeled rhPSMA Inhibitors. *J. Nucl. Med.* **2020**, *61*, 735–742.
- (33) Oh, S. W.; Wurzer, A.; Teoh, E. J.; Oh, S.; Langbein, T.; Krönke, M.; Herz, M.; Kropf, S.; Wester, H.-J.; Weber, W. A.; Eiber, M. Quantitative and Qualitative Analyses of Biodistribution and PET Image Quality of a Novel Radiohybrid PSMA,  $^{18}\text{F}$ -rhPSMA-7, in Patients with Prostate Cancer. *J. Nucl. Med.* **2020**, *61*, 702–709.
- (34) Kuo, H.-T.; Lin, K.-S.; Zhang, Z.; Uribe, C. F.; Merkens, H.; Zhang, C.; Benard, F. Novel  $^{177}\text{Lu}$ -labeled Albumin-binder-conjugated PSMA-targeting Agents with Extremely High Tumor Uptake and Enhanced Tumor-to-kidney Absorbed Dose Ratio. *J. Nucl. Med.* **2020**, DOI: 10.2967/jnumed.120.250738.
- (35) Kramer, V.; Fernández, R.; Lehnert, W.; Jiménez-Franco, L. D.; Soza-Ried, C.; Eppard, E.; Ceballos, M.; Meckel, M.; Benešová, M.; Umbricht, C. A.; Kluge, A.; Schibli, R.; Zhernosekov, K.; Amaral, H.; Müller, C. Biodistribution and dosimetry of a single dose of albumin-binding ligand [ $^{177}\text{Lu}$ ]Lu-PSMA-ALB-56 in patients with mCRPC. *Eur. J. Nucl. Med. Mol. Imaging* **2020**, DOI: 10.1007/s00259-020-05022-3.
- (36) Singh, A. N.; Dakanali, M.; Hao, G.; Ramezani, S.; Kumar, A.; Sun, X. Enantiopure bifunctional chelators for copper radiopharmaceuticals - Does chirality matter in radiotracer design? *Eur. J. Med. Chem.* **2014**, *80*, 308–315.
- (37) Podilapu, A. R.; Kulkarni, S. S. First synthesis of Bacillus cereus Ch HF-PS cell wall trisaccharide repeating unit. *Org. Lett.* **2014**, *16*, 4336–4339.
- (38) Liu, C.; Hasegawa, K.; Russell, S. J.; Sadelain, M.; Peng, K. W. Prostate-specific membrane antigen retargeted measles virotherapy for the treatment of prostate cancer. *Prostate* **2009**, *69*, 1128–1141.
- (39) Current, K.; Meyer, C.; Magyar, C. E.; Mona, C. E.; Almajano, J.; Slavik, R.; Stuparu, A. D.; Cheng, C.; Dawson, D. W.; Radu, C. G.; Czernin, J.; Lueckerath, K. Investigating PSMA-Targeted Radioligand Therapy Efficacy as a Function of Cellular PSMA Levels and Intratumoral PSMA Heterogeneity. *Clin. Cancer Res.* **2020**, *26*, 2946–2955.
- (40) Hillier, S. M.; Maresca, K. P.; Femia, F. J.; Marquis, J. C.; Foss, C. A.; Nguyen, N.; Zimmerman, C. N.; Barrett, J. A.; Eckelman, W. C.; Pomper, M. G.; Joyal, J. L.; Babich, J. W. Preclinical evaluation of novel glutamate-urea-lysine analogues that target prostate-specific membrane antigen as molecular imaging pharmaceuticals for prostate cancer. *Cancer Res.* **2009**, *69*, 6932–6940.
- (41) Eisenwiener, K.-P.; Prata, M. I. M.; Buschmann, I.; Zhang, H.-W.; Santos, A. C.; Wenger, S.; Reubi, J. C.; Mäcke, H. R. NODAGATOC, a new chelator-coupled somatostatin analogue labeled with [ $^{67/68}\text{Ga}$ ] and [ $^{111}\text{In}$ ] for SPECT, PET, and targeted therapeutic applications of somatostatin receptor (hsst2) expressing tumors. *Bioconjugate Chem.* **2002**, *13*, 530–541.
- (42) Levy, S. G.; Jacques, V.; Zhou, K. L.; Kalogeropoulos, S.; Schumacher, K.; Amedio, J. C.; Scherer, J. E.; Witowski, S. R.; Lombardy, R.; Koppetsch, K. Development of a Multigram Asymmetric Synthesis of 2-(R)-2-(4,7,10-Tris tert-Butylcarboxymethyl-1,4,7,10-tetraazacyclododec-1-yl)-pentanedioic Acid, 1-tert-Butyl Ester, (R)-tert-Bu4-DOTAGA(1). *Org. Process Res. Dev.* **2009**, *13*, 535–542.
- (43) Kielar, F.; Tei, L.; Terreno, E.; Botta, M. Large relaxivity enhancement of paramagnetic lipid nanoparticles by restricting the local motions of the  $\text{Gd}^{\text{III}}$  chelates. *J. Am. Chem. Soc.* **2010**, *132*, 7836–7837.
- (44) Henig, J.; Tóth, É.; Engelmann, J.; Gottschalk, S.; Mayer, H. A. Macrocyclic  $\text{Gd}^{3+}$  chelates attached to a silsesquioxane core as potential magnetic resonance imaging contrast agents: synthesis, physicochemical characterization, and stability studies. *Inorg. Chem.* **2010**, *49*, 6124–6138.
- (45) Ndiaye, M.; Malytskyi, V.; Vangijzegem, T.; Sauvage, F.; Wels, M.; Cadiou, C.; Moreau, J.; Henoumont, C.; Boutry, S.; Muller, R. N.; Harakat, D.; De Smedt, S.; Laurent, S.; Chuburu, F. Comparison of MRI Properties between Multimeric DOTAGA and DO3A Gadolinium-Dendron Conjugates. *Inorg. Chem.* **2019**, *58*, 12798–12808.
- (46) Moreau, J.; Guillon, E.; Pierrard, J. C.; Rimbault, J.; Port, M.; Aplincourt, M. Complexing mechanism of the lanthanide cations  $\text{Eu}^{3+}$ ,  $\text{Gd}^{3+}$ , and  $\text{Tb}^{3+}$  with 1,4,7,10-tetrakis(carboxymethyl)-1,4,7,10-tetraazacyclododecane (dota)-characterization of three successive complexing phases: study of the thermodynamic and structural properties of the complexes by potentiometry, luminescence spectroscopy, and EXAFS. *Chemistry* **2004**, *10*, 5218–5232.
- (47) Moreau, J.; Guillon, E.; Aplincourt, P.; Pierrard, J. C.; Rimbault, J.; Port, M.; Aplincourt, M. Thermodynamic and Structural Properties of  $\text{Eu}^{3+}$ ,  $\text{Gd}^{3+}$  and  $\text{Tb}^{3+}$  Complexes with 1, 4, 7, 10-Tetra (2-glutaryl)-1, 4, 7, 10-tetraazacyclododecane in Solution: EXAFS, Luminescence, Potentiometric Studies, and Quantum Calculations. *Eur. J. Inorg. Chem.* **2003**, *2003*, 3007–3020.
- (48) Kung, H.; Choi, S. R.; Zha, Z.; Ploessl, K.; Alexoff, D. [ $^{68}\text{Ga}$ ]/[ $^{177}\text{Lu}$ ] P17-087: A potential theranostic agent targeting PSMA expressing tumor. *JOURNAL OF LABELLED COMPOUNDS & RADIOPHARMACEUTICALS*; 2019; pp. S99-S100.
- (49) Benešová, M.; Bauder-Wüst, U.; Schäfer, M.; Klika, K. D.; Mier, W.; Haberkorn, U.; Kopka, K.; Eder, M. Linker Modification Strategies To Control the Prostate-Specific Membrane Antigen (PSMA)-Targeting and Pharmacokinetic Properties of DOTA-Conjugated PSMA Inhibitors. *J. Med. Chem.* **2016**, *59*, 1761–1775.